Quaternary Science Reviews 264 (2021) 107008

Contents lists available at ScienceDirect

Quaternary Science Reviews

journal homepage: www.elsevier.com/locate/quascirev

Summer temperatures during the last glaciation (MIS 5c to MIS 3) inferred from a 50,000-year chironomid record from Füramoos, southern Germany

Alexander Bolland [a, *], Oliver A. Kern [b], Frederik J. Allstädt [b], Dorothy Peteet [c], Andreas Koutsodendris [b], Jörg Pross [b], Oliver Heiri [a]

[a] Geoecology, Department of Environmental Sciences, University of Basel, Klingelbergstrasse 27, CH-4056, Basel, Switzerland
[b] Paleoenvironmental Dynamics Group, Institute of Earth Sciences, Heidelberg University, Im Neuenheimer Feld 234, D-69120, Heidelberg, Germany
[c] Lamont-Doherty Earth Observatory, Palisades, NY, USA

ARTICLE INFO

Article history:
Received 25 January 2021
Received in revised form
25 May 2021
Accepted 28 May 2021
Available online xxx

Handling Editor: Yan Zhao

Keywords:
Chironomids
Central Europe
Palaeoecology
Palaeoclimate
Summer temperature
Würmian glaciation
Last glacial Period

ABSTRACT

There is a sparsity of long, continuous palaeotemperature records for the last glacial period in central Europe, particularly for the interval corresponding to Marine Isotope Stages (MIS) 4 and 3. Here we present a new, ca. 50-thousand year (ka)-long chironomid record from Füramoos, southern Germany, covering the interval from MIS 5a to MIS 3 that we use to examine lake development and then to quantitatively reconstruct mean July air temperatures. Chironomid assemblages with high abundances of taxa such as *Polypedilum nubeculosum*-type, *Microtendipes pedellus*-type, *Cladopelma lateralis*-type and *Dicrotendipes nervosus*-type imply a shallow-lake setting for the majority of the examined interval, which is corroborated by other aquatic remains such as oribatid mites, Sialidae and Ceratopogonidae. Assemblages from the interval ca. 99 to 80 ka (in the region corresponding to the Brörup Interstadial, Stadial B and early Odderade Interstadial) are dominated by taxa such as *Tanytarsus glabrescens*-type and *Tanytarsus mendax*-type and indicate relatively warm temperatures. Assemblages from the interval covering ca. 80 to 54 ka (corresponding to the late Odderade, Stadial C, Dürnten Interstadial and Stadial D) are dominated by taxa such as *Sergentia coracina*-type and *Tanytarsus lugens*-type and are typical for cooler conditions. Reconstructed July temperatures for the early Würmian (Brörup to early Odderade; ca. 99–80 ka) are 13–14 °C. Values decline to <10 °C during the late Odderade and Stadial C (ca. 80–77 ka) around the MIS 5a/4 transition. This decrease is coeval with a pronounced decrease in Northern Hemisphere summer insolation. Values stay in the range of 9–11 °C during the Dürnten and Stadial D (ca. 54–74.5 ka) and increase again to 12.5 °C during the Bellamont 1 interstadial (ca. 54–46 ka). Reconstructed July temperatures track changes in arboreal pollen percentages at Füramoos and agree with a summer-temperature decrease during the early to mid-Würmian as reported by other palaeotemperature records from Europe and the North Atlantic. Our chironomid record from Füramoos provides valuable new insights into Würmian climate dynamics in Central Europe, and corroborates other temperature reconstructions from the early to mid-Würmian glacial period.

1. Introduction

The Last Glacial Period (in southern Central Europe referred to as the Würmian Glaciation) is dated to ca. 115–11.7 ka ago (Imbrie et al., 1984; Shackleton et al., 2003; Lowe et al., 2008; Ivy-Ochs et al., 2008) beginning in Marine Isotope Stage (MIS) 5d and ending in the first part of MIS 1 with the onset of the Holocene. It was characterized by major glaciation on the continents (Hughes et al., 2013; Hughes and Gibbard, 2018), an associated decrease in sea level (Waelbroeck et al., 2002; Spratt and Lisiecki, 2016), a general trend to increased continentality (Caspers and Freund, 2001; Helmens, 2014), and distinct centennial-to millennial-scale changes in terrestrial ecosystems, notably vegetation (Behre and Lade, 1986; Woillard, 1978; Müller et al., 2003; Fletcher et al., 2010). Over large parts of Europe, vegetation changed from the

* Corresponding author.
E-mail address: alexanderwilliam.bolland@unibas.ch (A. Bolland).

https://doi.org/10.1016/j.quascirev.2021.107008

forested conditions of the last interglacial to tundra or steppe vegetation during the coldest phases of the last glaciation (Behre and Lade, 1986; Woillard, 1978; Müller et al., 2003; Fletcher et al., 2010). During the last glacial period, climate in the North Atlantic region was also associated with a number of rapid, centennial-scale cooling and warming events (stadials and interstadials). In Greenland ice core $\delta^{18}O$ records, 26 stadials and 25 interstadials are documented between the current and the last interglacial (Dansgaard et al., 1993; Rasmussen et al., 2014). Several of these events have been detected in stable-isotope data from speleothems in Europe particularly for the early/mid-Würmian ca. 115–60 ka (Boch et al., 2011; Moseley et al., 2020) and have been correlated to distinct vegetation changes on the European continent (e.g., Woillard, 1978; Müller et al., 2003; Fletcher et al., 2010 and references therein). Importantly, however, not all Greenland interstadials appear to be associated with corresponding vegetation changes possibly due to plant-migration lags (Müller et al., 2003; Fletcher et al., 2010; Helmens, 2014).

Quantitative palaeotemperature records play an important role for understanding climatic and environmental changes during the last glaciation. They can be used to assess the performance of climate models (e.g., Renssen and Isarin, 2001; Heiri et al., 2014) and are also necessary for assessing, and in some cases modelling the impact of past climatic changes on vegetation, landscape and glacier dynamics (Hubbard et al., 2006; Lischke et al., 2013; Seguinot et al., 2018). However, continuous centennial to millennial scale palaeotemperature reconstructions that cover long continuous time intervals of the last glaciation are rare for Europe north of the Alps. Vegetation-based reconstructions are available for the long pollen records of Samerberg, Jammertal, Füramoos, Les Echets (Klotz et al., 2004) and Gröbern (Kühl et al., 2007, Fig. 1), usually providing information on summer temperature, winter temperature and/or changes in humidity. Beetle-based reconstructions of the mean temperatures of the coldest and warmest months have been derived from La Grande Pile (Ponel, 1995) in eastern France as well as Gröbern (Walkling and Coope, 1996) and Oerel (Behre et al., 2005) in northern Germany (Fig. 1).

Important quantitative information on past climatic conditions has also become available through the analysis of chironomids, a group of aquatic insects whose larval remains preserve well in lake sediments and can be identified to the generic or morphological type level (Brooks et al., 2007). The distribution of chironomid assemblages in lakes is closely related with summer temperatures (Eggermont and Heiri, 2012), and fossil chironomid analysis has been used to develop quantitative summer-temperature reconstructions (Langdon et al., 2008; Luoto, 2009a, 2009b, 2009b; Larocque et al., 2001; Heiri et al., 2003b, 2011). This approach has been followed to reconstruct past summer temperature changes during the Lateglacial (e.g., Brooks and Birks, 2000; Heiri and Millet, 2005; Tóth et al., 2012; Bolland et al., 2020). However, only very few records, usually representing only sections of the last glacial period are available for earlier parts of the Würmian glaciation. Notable examples come from eastern Germany (MIS 3: Engels et al., 2008), northern Italy (Last Glacial Maximum: Samartin et al., 2012), Austria (MIS 5a: Ilyashuk et al., 2020) and Northern Finland (MIS 5d–c, MIS 3; Helmens et al., 2009, 2012; Engels et al., 2010, 2014). While these records provide valuable information for the examined time intervals, they represent fragmented intervals of the last glacial period. Thus, they do not allow the assessment of long-term, multi-millennial-scale changes in ecosystem or climatic development.

Here we provide the first millennial- to centennial-scale resolution chironomid-based temperature reconstruction covering a ca. 50,000-years-long, continuous interval of the last glacial period from the classical site of Füramoos, southern Germany. Our new record covers the interval from MIS 5c to MIS 3 (ca. 99–46 ka) in the region representing the Brörup Interstadial, Stadial B, Odderade Interstadial, Stadial C, Dürnten Interstadial, Stadial D, and Bellamont 1, a middle Würmian interstadial named after a village local to Füramoos (Müller et al., 2003). We provide details regarding the correlation of these stadials and interstadials to MIS stages, GIS stages and Würmian interstadials/stadials as described in other records (and referred to in the discussion) in Supplementary Information 1. Over the course of the study interval there is widespread evidence of increasing continentality connected to climatic cooling across Central and Northern Europe (Caspers and Freund, 2001; Helmens, 2014). As such, the new record contributes to better understanding the magnitude, timing and effects of climate change during the last glacial period in Central Europe.

2. Methodology

2.1. Site description and coring

Füramoos Ried is a peat bog covered by a modern forest in southern Germany's alpine foreland, a region with modern mean July air temperatures of 16–18 °C for the period 1961–1990 (https://www.dwd.de). A mean July air temperature value of 17.8 °C was recorded 1991–2020 at 610–615 m above sea level (asl) at Memmingen, ca 20 km from Füramoos (DWD Climate Data Centre, 2021). The bog is formed in a 1100 m long and 600 m wide basin, and situated at 662 m asl between two Rissian glacial moraines (Schreiner, 1996; Busschers et al., 2008) preserving a near-continuous record of environmental change from the end of the previous glaciation (locally referred to as the Rissian Glaciation; equivalent to MIS 8–6) to the onset of the Holocene (Schreiner, 1981; Müller et al., 2003; Winterholler, 2004; Kern et al., 2019). Previous analysis at this site include vegetation reconstructions, organic matter profiles, X-ray fluorescence (XRF) measurements and correlations to other palaeoecological and palaeoclimatological records (Müller et al., 2003; Kern et al., 2019). Our study is based on three sediment cores termed FU1, FU3, and FURA that cover different portions of the limnotelmatic succession deposited in the Füramoos Ried. The cores FU1 and FU3 were taken at 47°59′32.474″ N, 9°53′13.905″ E within a horizontal distance of 1.5 m using a Wacker Neuson BH-65 drill hammer (inner core diameter: 5 cm) (Kern et al., 2019). The FURA core was collected in 2001 at 47°59′26.9″ N 9°53′10.1″ E using a mobile drilling rig and has an inner diameter of 10 cm.

The cores FU1 and FU3 were correlated based on (XRF) core scanning data (Ca normalized to total counts). The FU1/3 core sequence was correlated to the FURA core based on XRF data (Ti:Al ratio) and supported by Loss on Ignition (LOI) data.

2.2. Pollen analysis

For palynological analyses, a sediment volume of 1–3 cm^3 was used per sample. *Lycopodium* tablets were added before chemical treatment for estimation of pollen concentrations (Stockmarr, 1971). Sample processing followed Eisele et al. (1994) and comprised treatment with 10% HCl, 10% NaOH and 40–45% HF, followed by acetolysis. Samples with high concentrations of clastic material were subjected to density separation using sodium polytungstate. Residues were embedded in “Kaiser's glycerine jelly”, fixed on microscope slides and analysed with a Carl Zeiss Axio Scope A1® microscope (400–1000× magnification) at the Institute of Earth Science, Heidelberg University. *Ranunculus aquatilis* (Müller et al., 2003) is included in *Ranunculus acris*-type, following Beug (2004). The pollen results are used here to confirm the correlation of the sediment cores and ensure a reliable correlation of

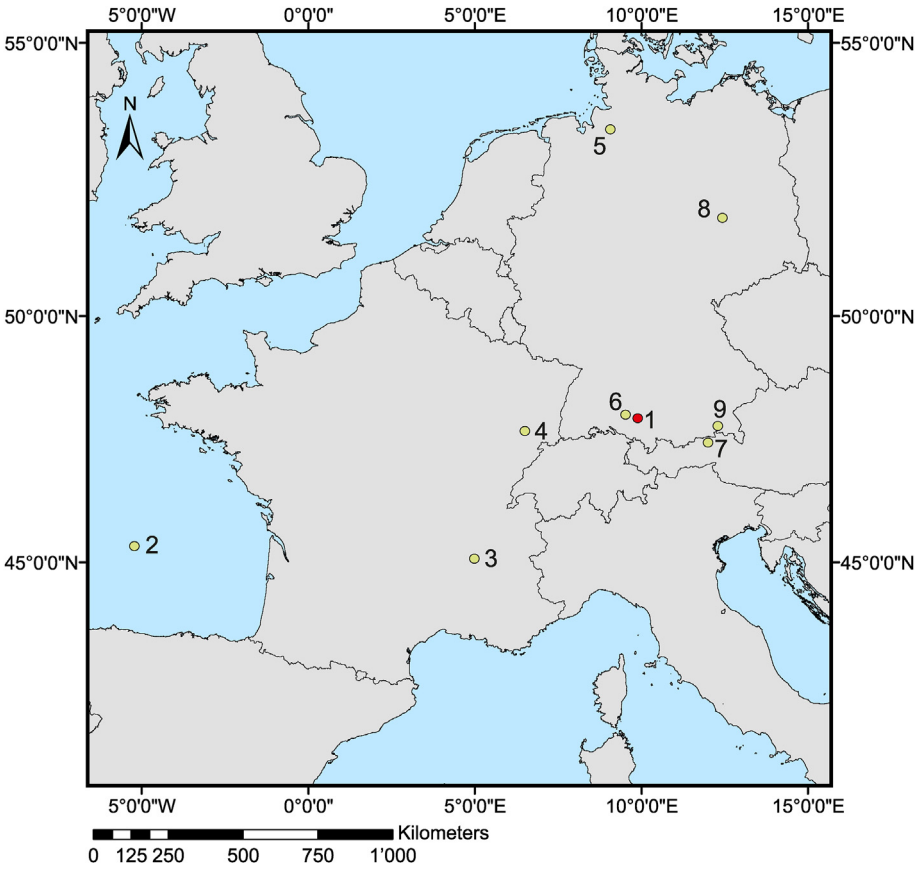

Fig. 1. Locations of the records that have been used to produce temperature reconstructions referred to in the text: 1. Füramoos (red circle; Müller et al., 2003; this study); 2. Core MD04-2845 (Sánchez Goñi et al., 2008, 2013); 3. Les Echets (de Beaulieu and Reille, 1984, 1989, 1989); 4. La Grande Pile (Woillard, 1978); 5. Oerel (Behre and Lade, 1986; Behre, 1989; Behre and van der Plicht, 1992; Behre et al., 2005); 6. Jammertal (Müller, 2000); 7. Unterangerberg (Ilyashuk et al., 2020); 8. Gröbern (Litt, 1994; Walkling and Coope, 1996); 9. Samerberg (Grüger, 1979). (For interpretation of the references to colour in this figure legend, the reader is referred to the Web version of this article.)

the study results to the sequence described by Müller et al. (2003) and will be described in detail elsewhere.

2.3. X-ray fluorescence core scanning and LOI

X-ray fluorescence core scanning was performed on all cores at the Institute of Earth Sciences, Heidelberg University using an Avaatech (GEN-4) XRF core scanner. In this study we use normalized Ca and the ratio of Ti/Al to correlate the FU1, FU3 and FURA sediment cores. A 10 kV Rh anode X-ray tube without a filter was used with a spatial resolution of 5 mm, a counting time of 10 s, a 150 mA current, and a slit size of 10 mm crosscore and 5 mm downcore. A 4-μm-thick Ultralene® foil was placed over the core halves after they were smoothed for analysis to avoid core desiccation and contamination of the detector window. The bAxilBatch software (Version 1.4, July 2016; www.brightspec.be) was used to process the X-ray spectra.

Sedimentary organic matter content measurements were taken every 4 cm in both the FURA and FU1/3 cores using LOI at 550 °C (Heiri et al., 2001). Analysis was conducted at the Institute of Earth Science, Heidelberg University.

2.4. Lithology and dating

Based on the lithology, coring depth and palynological information, the cores FU1 and FU3 mainly cover the late early Würmian to middle Würmian, and the FURA core covers the interval from the Rissian Lateglacial to the middle Würmian (sensu Chaline and Jerz, 1984 in Preusser, 2003). The analysis in this study focuses on the younger section from 12.90 to 4.67 m from the Brörup interstadial onwards.

Müller et al. (2003) developed an age-depth model for their core from Füramoos by aligning the pollen record from that core with palaeoclimate records from the North Atlantic (McManus et al., 1994) and Greenland (Dansgaard et al., 1993). This allowed the placement of the pollen record within the marine isotope stratigraphy (Martinson et al., 1987). Our new Füramoos composite record was correlated to the record of Müller et al. (2003) based on pollen assemblages, tied at the onset of each of the following time intervals: Brörup, Stadial B, Odderade, Stadial C, Dürnten, Stadial D, Bellamont 1 and Stadial E (Fig. 2). The ages of the onset of each of these intervals as reported in Müller et al. (2003) were used to provide an age assessment of our Füramoos composite core. According to this correlation, the sediment sections of the present study cover the time interval from Greenland interstadial (GIS) 23, correlated to the middle of the Brörup interstadial, to Greenland interstadials (GIS) 13 and 14, correlated with the Bellamont 1 interstadial (Müller et al., 2003). Thus, they represent the time interval from the later part of MIS 5 to early MIS 3.

2.5. Chironomid sample preparation and analysis

Forty-six samples were selected for chironomid analysis from the FURA cores (12.91–9.14 m composite depth) and 71 samples from the FU1/FU3 cores (9.24–4.67 m composite depth; Fig. 2). The incorporation of the FURA core into the composite core and

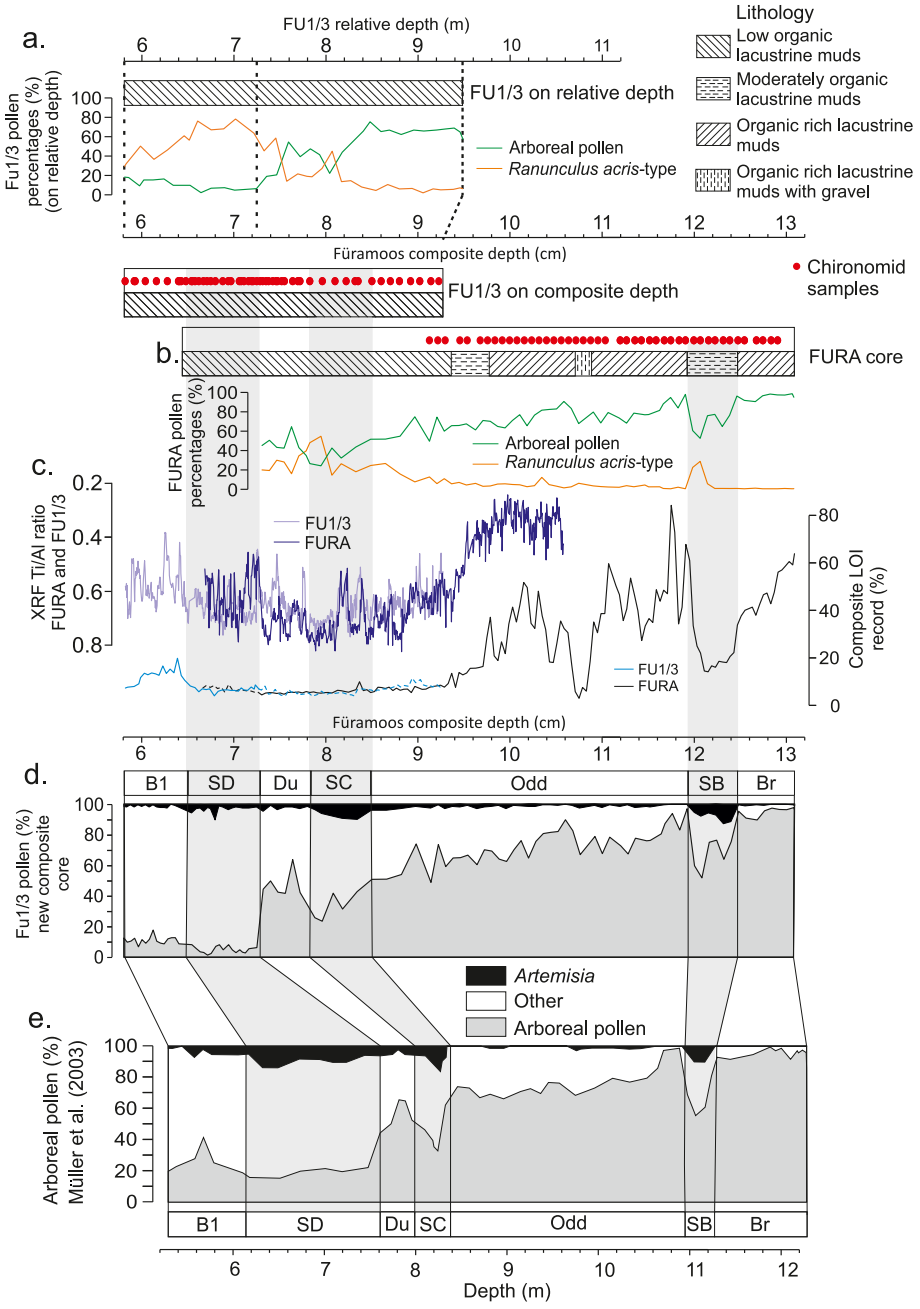

Fig. 2. Correlation diagram illustrating how the composite core was produced from the FU1/FU3 and FURA cores, and how the composite core was correlated to the pollen record of Müller et al. (2003). Selected data are displayed for presentation purposes. a. Lithology, % arboreal pollen and % *Ranunculus acris*-type as well as position of chironomid samples in the FU1/FU3 cores plotted both on relative coring depth and composite coring depth. b. Lithology, % arboreal pollen and % *Ranunculus acris*-type as well as position of chironomid samples in the FURA core plotted on composite depth. c. Ti/Al ratio based on XRF analyses as well as Loss on Ignition (LOI) data from FU1/FU3 and FURA cores plotted against composite depth. d. Arboreal pollen and *Artemisia* pollen percentages for the new composite record plotted on composite depth as well as position of stadials and interstadials in the new record identified based on stratigraphic data (FURA pollen data from 14.28 to 7.32 to m composite depth and FU1/3 pollen data from 7.27 to 4.66 m). e. Pollen data and position of stadials and interstadials in the record of Müller et al. (2003) plotted on original depth scale of this record. Br: Brörup, SB: Stadial B, Odd: Odderade, SC: Stadial C, Du: Dürnten, SD: Stadial D, B1: Bellamont 1.

subsequent re-evaluation of the chronology has resulted in an uneven sampling distribution of chironomid samples, ranging from one sample every 2 cm to every 12 cm with some exceptions. Sediment volume ranged between 0.5 and 10.3 cm^3 per sample depending on chironomid concentrations. Samples above 9.6 m required no chemical pre-treatment. Samples below 9.60 m were heated in 10% KOH for 15 min at 85 °C due to sediment compaction and difficulty sieving the compact organic sediments. Samples were sieved with 100 μm mesh-size, and chironomid head capsules as well as other chitinous aquatic invertebrate remains were picked from a Bogorov tray under a stereomicroscope (30–50× magnification). Samples were then dried and mounted in Euparal before identification at 40–100× magnification using a compound microscope. A minimum head capsule count of 80 was aimed for to produce more than the recommended 50 head capsules per sample (Heiri and Lotter, 2001). Head capsules with a complete mentum or greater than half a mentum were counted as one specimen, head capsules with half a mentum were counted as half a specimen and

head capsules with less than half a mentum were disregarded. Next to chironomids the remains of Sialidae, Ceratopogonidae, *Daphnia*, Ephemeroptera, oribatid mites, Trichoptera, Plecoptera, Sciaridae and Tipulidae as well as Characeae oogonia and *Plumatella* statoblasts were mounted and identified.

2.6. Chironomid identification

Taxonomic identification followed Wiederholm (1983), Schmid (1993), Brooks et al. (2007), and Anderson et al. (2013). Specimens not identified to a sufficient taxonomic level (e.g. unidentified Chironomini) were excluded from further analysis. Some sections of the record contained a relatively large number of damaged *Tanytarsus*-type head capsules with broken antennal pedestals and missing mandibles presumably due to the difficulty separating them from the amorphous organic matter in the samples. *Tanytarus pallidicornis*-type and *Tanytarsus mendax*-type, are not possible to split without preserved antennal pedestals. However, as identified specimens of *Tanytarsus mendax*-type were far more abundant throughout the record than identified *Tanytarsus pallidicornis*-type, ambiguous specimens were assigned to *Tanytarsus mendax*-type. Similarly, *Tanytarsus lugens*-type and *Tanytarsus mendax*-type are difficult to differentiate without mandibles. However, within the record *Tanytarsus lugens*-type specimens identified with mandibles were consistently more darkly pigmented than *Tanytarsus mendax*-type specimens identified with mandibles. In many cases we were therefore able to differentiate these two types based on pigmentation and remaining ambiguous specimens, "*Tanytarsus lugens/mendax*-type", were then split based on the ratio of identified *Tanyrtarsus lugens*-type and *Tanytarsus mendax*-type in every sample that they occurred. Overall the ratio of identified *Tanyrtarsus lugens*-type and *Tanytarsus mendax*-type to the "*Tanytarsus lugens/mendax*-type" category was 6.7 : 1. Remains of Sialidae, Ceratopogonidae, Ephemeroptera, Trichoptera, Plecoptera, Sciaridae and Tipulidae were identified to this taxonomic level based on a photo collection of mounted modern specimens at Geoecology, University of Basel (Courtney-Mustaphi et al. in preparation), oribatid mites based on descriptions in Solhøy (2001) and Characeae oogonia based on Haas (1994). *Daphnia* and *Plumatella* were identified to morphological types based on Vandekerkhove et al. (2004) and Francis (2001).

2.7. Zonation and ordination analysis

The clustering algorithm CONISS (Grimm, 1987) was used to determine zonations in the chironomid record that were subsequently tested for statistical significance using a Broken Stick Model (Bennett, 1996). R studio version 1.1.463 (RStudio Team, 2015) was used to calculate CONISS using the *rioja* (Juggins, 2017) package. A Detrended Correspondence Analysis (DCA) was used to summarize major changes in the chironomid assemblage using CANOCO 5 (Šmilauer and Leps, 2014). These numerical analyses were based on square root transformed percentage data.

2.8. Temperature reconstruction

A chironomid-based temperature reconstruction was produced using a chironomid-temperature calibration dataset and temperature inference model based on surface-sediment samples from 274 Swiss and Norwegian lakes (Heiri et al., 2011) A two-component weighted averaging partial least squares model (WAPLS; ter Braak and Juggins, 1993; ter Braak et al., 1993) was used to estimate mean July air temperatures from fossil assemblages. The model featured a root mean square error of prediction of 1.42 °C and an r^2 of 0.90 between predicted and observed temperatures when assessed using bootstrapping within the calibration dataset. In the Füramoos record some samples were aggregated with their adjacent samples to achieve higher numbers of chironomids per sample (minimum: 40 head capsules), resulting in a total of 75 chironomid samples of the original 93 samples where chironomids were present. Of the original 73 types identified, some had to be aggregated, and one type, i.e., *Constempellina − Thienemanniola*, was excluded since it was not represented in the calibration data, resulting in 67 types used in total. Percentages were square root transformed prior to the calculations.

Squared chi-square distance was used to identify assemblages with either "no close" or "no good" modern analogues (Birks et al., 1990) in the modern calibration set, with thresholds for identifying such samples set as the 2nd and 5th percentiles of all distances within the modern calibration data samples, respectively (Birks et al., 1990; Tóth et al., 2015). A Canonical Correspondence Analysis (CCA) of the calibration dataset was produced with the fossil data analysed as passive samples and the only constraining variable set as mean July air temperature. The 90th and 95th percentile of residual distances of the modern calibration dataset samples to axis 1 were used to determine samples in the fossil record with a "poor" and "very poor" "goodness of fit" to temperature respectively (Birks, 1990; Tóth et al., 2015). Furthermore, sample specific estimated standard errors of prediction were calculated by using bootstrapping (9999 cycles, Birks et al., 1990) and the percentage of taxa absent from the training set as well as the number of rare taxa (N2<5 in the calibration dataset;(Heiri et al., 2003b) in the samples was calculated. C2 Version 1.7.7 was used to calculate analogue statistics (Juggins, 2007) and CANOCO 5 was used to produce the CCA (ter Braak and Smilauer, 2018). Analyses were based on square root transformed percentages.

3. Results

3.1. Würmian chironomid record

The new chironomid record consists of 75 chironomid samples that contained large enough chironomid counts to use in analysis following omission of samples with no chironomids and the joining of samples with fewer than 40 headcapsules (Fig. 3). CONISS zonation identified four statistically significant breaks in the chironomid record, resulting in five chironomid zones: Chironomid Zone Füramoos (CZF) 1 through 5. From the 115 samples originally processed for chironomid analysis 22 samples did not contain enough chironomid remains to be used.

CZF 1 (12.91−12.07 m) contains two intervals in which *Dicrotendipes nervosus*-type and *Microtendipes pedellus*-type dominate, respectively. *Chironomus anthracinus*-type and *Polypedilum nubeculosum*-type are subdominant in this section. Sialidae and *Cladopelma lateralis*-type are at their highest abundances in the entire record in CZF 1, but decline in abundance throughout the zone. CZF 2 (12.07−9.70 m) is dominated by *Corynocera ambigua* and, to a lesser extent, by *Chironomus anthracinus*-type throughout the zone. A subtle shift in chironomid assemblages is observed in this zone with types such as *Tanytarsus glabrescens*-type only occurring in the first part and then disappearing while other types, such as *Tanytarsus lugens*-type and *Sergentia coracina*-type occur intermittently before increasing in abundance towards the end. High abundances of Ceratopogonidae and oribatid mites are a prominent feature of CZF 2, and Sialidae remain present in this zone, but are less abundant relative to CZF 1. Within CZF 3 (9.70−6.84 m), *Chironomus anthracinus*-type and *Corynocera ambigua* remain in relatively high abundance, but are joined by increasing abundances of *Tanytarsus lugens*-type and *Sergentia coracina*-type, all four types becoming co-dominant. Many of the remains that were present in CZF 2

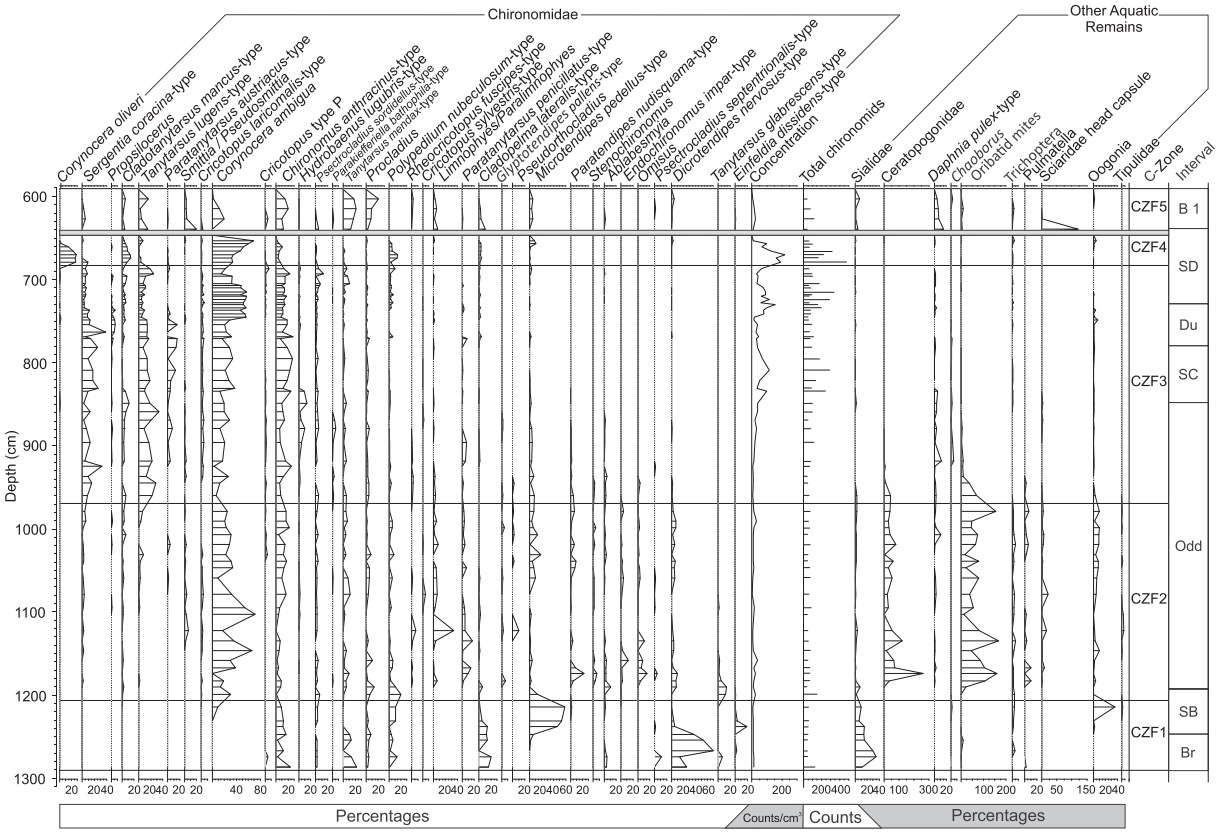

Fig. 3. Distribution of chironomids in the Füramoos composite record plotted against composite depth. Chironomid remains are displayed as a percentage of total identified chironomids. C-zone is Chironomid Zone determined by CONISS zonation. Other aquatic remains are displayed as a percentage relative to total chironomids including those that were not identified at higher taxonomic resolution. Chironomid types below 5% in the record are not shown (41 types). Chironomid types are ordered according to abundance weighted average depth of occurrence, with types more abundant at the top of the core displayed on the left and those more abundant at the bottom displayed on the right. The grey horizontal bar indicates a sediment section without chironomids (see text for details). Br: Brörup, SB: Stadial B, Odd: Odderade, SC: Stadial C, Du: Dürnten, SD: Stadial D, B1: Bellamont 1.

persist into the earliest section of CZF 3, such as *Paratendipes nudisquama*-type, oribatid mites and Ceratopogonidae, but decline and disappear shortly after the transition. The main distinguishing feature of CZF 4 (6.84–6.54 m) is the dominance of *Corynocera oliveri*. *Sergentia coracina*-type disappears and *Tanytarsus lugens*-type decreases in abundance, whereas *Corynocera ambigua* persists at high abundances. The highest concentration of chironomids are found in CZF 4. CZF 4 and CZF 5 are separated by an interval in which no chironomids and only a single Sciaridae head capsule were found. The beginning of CZF 5 (6.40–6.04 m) coincides with an increase in chironomid concentrations to useable levels with initial high abundances of *Smittia/Pseudosmittia* as well as Sciaridae. *Corynocera ambigua*, *Chironomus anthracinus*-type, *Procladius* and *Tanytarsus mendax*-type dominate in this zone, and *Daphnia* ephippia are also abundant.

3.2. Chironomid-inferred temperature and ordination results

Chironomid-inferred July air temperatures within CZF 1 are relatively stable around 14 °C (Fig. 4). Within CZF 2 temperatures decrease to values around 12–13 °C, although this trend is interrupted by major short-term variations, including a single sample positive excursion to 18 °C (11.74 m) and two negative excursions consisting of one and three samples, respectively, to ca. 10.5 °C (11.47 m) and ca. 9–12 °C (11.03–10.79 m) in the middle of the zone. Within CZF 3, chironomid-inferred July air temperatures decrease in a stepwise fashion to 11 °C between 9.40 and 8.30 m, and then to 8.5 °C between 8.40 and 7.80 m before increasing and fluctuating between 9 and 11 °C for the rest of the zone. For CZF 4, temperatures are ca. 10.5 °C although the value for the final sample prior to the zone with no chironomids decreased to 9 °C. The final zone CZF 5 shows a temperature increase to 11–12 °C.

DCA Axis 1 and 2 explain 10.83% and 7.96% of the variance in the assemblage data, with axis lengths of 2.7 and 3.2 S.D., respectively (Fig. 4). There is a general shift for DCA Axis 1 to lower values along the record, from initial values of 2.25 to 0.5 S.D. after 7.50 m depth. In the youngest section values increase again to reach 1.5 S.D. at 6.04 m composite depth. Overall DCA Axis 1 appears to represent changes in chironomid-inferred temperature in the Füramoos composite core. DCA Axis 2 displays more marked changes than DCA Axis 1, increasing from 0.5 to 3.25 S.D. at the beginning of CZF 2 before decreasing to 2.0 to 2.5 S.D. and remaining stable until CZF 4 where S.D. units fall to 1. Following the chironomid-free zone, S.D. units increase again to 1.5 S.D.

Modern-analogue statistics indicate that overall most samples in the record have a good analogue in the calibration data (Fig. 4), although samples with close analogues are mainly restricted to CZF 3. However, within most zones, with the exception of CFZ 5, individual samples have no good analogues. Most samples have a good fit with temperature. However, there are two sections in the record (11.83–11.23 m and 7.69–7.35 m) where many of the samples have a poor or very poor fit with temperature. Taxa not represented in the training set were below 3% for the entire record. Abundances of rare taxa were generally below 8%, but some samples contained as

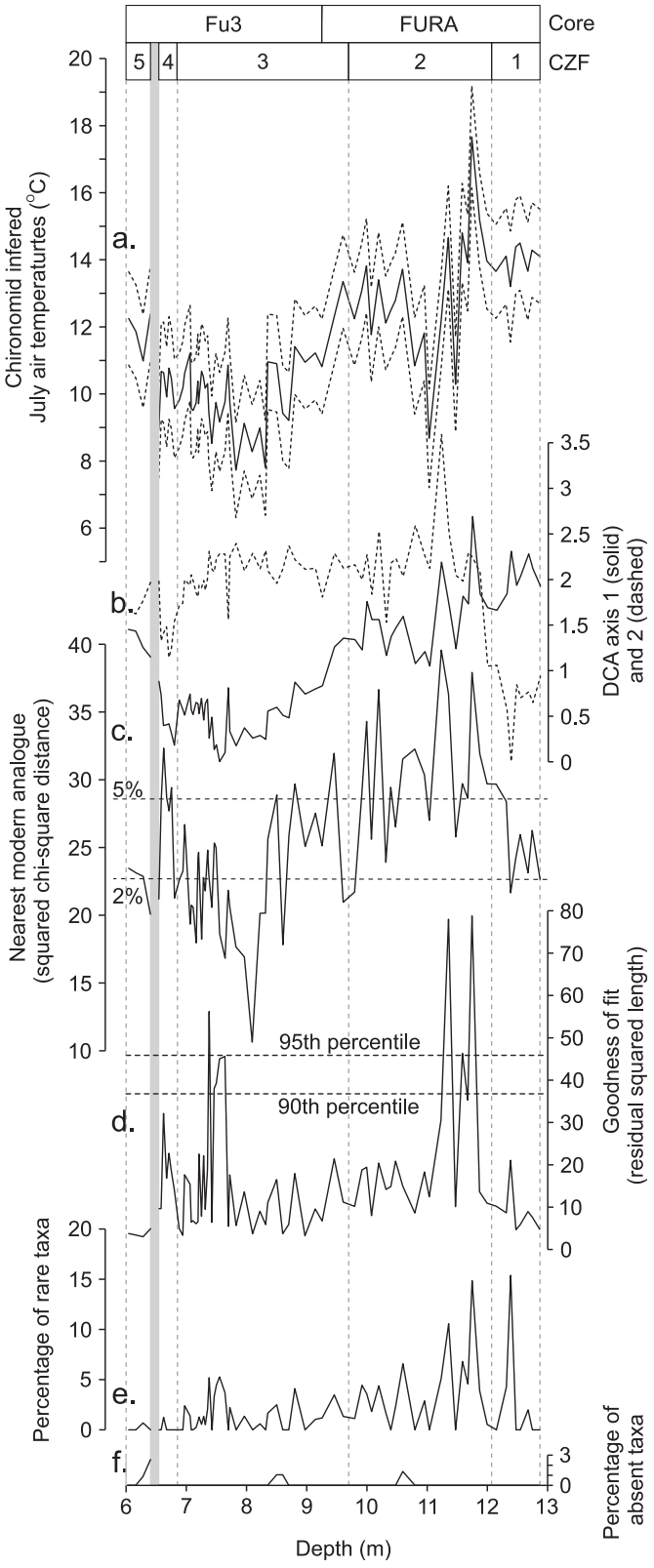

Fig. 4. Chironomid-inferred July air temperatures together with ordination results and associated diagnostic statistics from the Füramoos composite record. a. Chironomid-inferred July air temperatures (solid line) and associated error estimates (dashed lines); b. DCA axis 1 (solid line) and axis 2 (dashed line); c. Squared chi-square distance of fossil samples to the nearest modern analogue in the calibration dataset. Samples with no close (2%) and no good (5%) analogues in the modern calibration data are indicated by dashed horizontal lines (following Tóth et al., 2015); d. goodness of fit statistics. Samples with a "poor fit" or "very poor fit" at the 90th and 95th percentiles of all residual distances of the modern calibration dataset samples are indicated by the dashed horizontal lines, respectively; e. percentage of taxa in the Füramoos samples that are rare in the Swiss-Norwegian training set; f. percentage of taxa in the Füramoos samples that are absent from the Swiss-Norwegian training set. Grey bar indicates a short section between CZF 4 and 5 without chironomids.

many as 19% of rare taxa.

4. Discussion

4.1. Chironomid assemblage and lake development

Several chironomid taxa typical for lacustrine conditions persist over large sections of the studied interval and generally indicate conditions typical for a relatively shallow lake environment. For example, *Polypedilum nubeculosum*-type, *Microtendipes pedellus*-type, *Cladopelma lateralis*-type and *Dicrotendipes nervosus*-type can all be abundant in shallow-water environments (e.g., Beattie, 1982; Walker et al., 1991; Lods-Crozet and Lachavanne, 1994; Millet et al., 2007; Korhola et al., 2000; Nazarova et al., 2017; Tóth et al., 2019) and occur in temperate lowland to subarctic/subalpine lakes (e.g., Walker et al., 1991; Brooks and Birks, 2000; Heiri et al., 2011). Several common chironomids (e.g., *Tanytarsus mendax*-type, *Tanytarsus lugens*-type, *Chironomus anthracinus*-type, *Procladius*, *Sergentia coracina*-type) can also be found in deepwater environments beneath a thermally stratified water column; type specific oxygen requirements permitting (e.g., Saether, 1979). However, these taxa also colonize shallower sections of lake basins under suitable conditions (e.g., Porinchu and Cwynar, 2000; Hofmann, 2001; Nazarova et al., 2017; Tóth et al., 2019). For example, for *Tanytarsus lugens*-type and *Sergentia coracina*-type this is only possible in cool conditions (e.g., Brundin, 1949; Heiri et al., 2011). *Corynocera ambigua*, an abundant and in some sections dominating chironomid, is common in shallow-water settings, but also occurs in deep-water habitats in some stratified lakes (e.g., Heiri, 2004). The species has been reported to dominate in lakes with abundant characeans (e.g., Fjellberg, 1972; Brodersen and Lindegaard, 1999), but has also been considered a cold-indicator (Luoto, 2009a) common in sediments from the last glaciation (e.g., Hofmann, 1983a, 1983b; Gandouin et al., 2016). However, more recent evidence suggests that it may have a wider thermal tolerance and temperature range (Brodersen and Lindegaard, 1999). Shifts between these dominating chironomid morphotypes as well as variations in less abundant taxa and non-chironomid invertebrates suggest several changes in lake conditions at Füramoos.

CZF 1 (12.91–12.07 m; ca. 99–85 ka) corresponds with the later part of the Brörup interstadial (12.91–12.47 m; ca. 99–87 ka) and the first sections of the following Stadial B (12.47–12.07 m; ca. 87–84.5 ka), intervals associated with MIS 5c and b, respectively (Müller et al., 2003), and consists of two lithologically distinct units. Sediments associated with the Brörup interstadial are highly organic lacustrine muds whereas sediments associated with Stadial B are only moderately organic, with a higher inorganic content (Fig. 2). Those samples associated with the late Brörup interstadial (ca. 99–87 ka) were difficult to process as the compressed highly organic material expanded beyond the initial sample volume once soaked and sieved, a feature also identified by Behre et al. (2005) from similar sediments at Oerel. Within CZF 1 there is a distinct chironomid assemblage change at ca. 87 ka associated with the transition from the late Brörup interstadial (*Dicrotendipes nervosus*-type dominance) to Stadial B (*Microtendipes pedellus*-type dominance). McGarrigle (1980) showed that *Microtendipes pedellus*-type prefers lower sedimentary organic-matter content while *Dicrotendipes* seems to prefer sediments with decaying plant matter and/

or detrital leaves (Pope et al., 1999), suggesting that sediment composition may have influenced the assemblage. Furthermore, the removal of *Tanytarsus mendax*-type at this transition may indicate a cooling (Heiri et al., 2011). A shallow-water environment is supported by the persistent presence of Sialidae larvae, benthic predators indicative of littoral conditions and muddy lake bottoms (Lemdahl, 2000). Overall CZF 1 indicates a shallow and relatively productive lake that cooled and became less productive at the Brörup/Stadial B transition.

CZF 2 (12.07–9.70 m; ca. 85–70.5 ka), corresponding to the final part of Stadial B and the majority of the Odderade interstadial, is dominated by the taxon *Corynocera ambigua,* which has a wide ecological tolerance (Brodersen and Lindegaard, 1999). At the onset of CZF 2 the subdominant taxa are *Polypedilum nubeculosum*-type, *Tanytarus glabrescens*-type and *Microtendipes pedellus*-type, all of which imply a warm mesotrophic environment (Beattie, 1982; Heiri and Lotter, 2005; Langdon et al., 2006; Brooks et al., 2007). The invertebrate assemblage is characterised by a higher influence of remains originating from shallower sections of lakes that may suggest a shallower environment, a more structured or productive littoral zone or enhanced transport from the lake margins towards the center. This is typified by the high abundances of oribatid mites, which can be representative of both shallow aquatic and terrestrial environment in and around lakes (de la Riva-Caballero et al., 2010; Heggen et al., 2012), and Ceratopogonidae, which indicate relatively warm and shallow aquatic environments (Walker and MacDonald, 1995; Ilyashuk et al., 2005). *Limnophyes/Paralimnophyes,* often associated with shallow-water and sometimes semi-terrestrial conditions (Porinchu and Cwynar, 2000; Massaferro and Brooks, 2002; Millet et al., 2007; Nazarova et al., 2017), is also recorded. Larvae of Sciaridae, remains of which can be found regularly in this zone, are terrestrial (Heiri and Lotter, 2007) and suggest some inwash of terrestrial invertebrate remains. Therefore, it appears that for a large part of CZF 2 relatively low lake levels prevailed at the FURA coring location, although most encountered chironomid taxa are aquatic, indicating that the coring site was well within the lake. Towards the end of CZF 2, the abundances of oribatid mites and Ceratopogonidae decline indicating a reduced influence of the shallow littoral environment, while occurrences of *Sergentia coracina*-type and *Tanytarus lugens*-type increase, indicating relatively cool temperatures (Brooks et al., 2007; Frey, 1988; Heiri et al., 2011; Nazarova et al., 2017). Overall, CZF 2 indicates an initial warm period with a potential expansion of the littoral zone and subsequent gradual cooling.

CZF 3 (9.70–6.84 m; ca. 79.5–73.5 ka) corresponds to the end of the Odderade interstadial (9.70–8.49 m; ca. 79.5–77 ka), Stadial C (8.49–7.81 m; ca. 77–74.5 ka), the Dürnten interstadial (7.81–7.30 m; ca. 74.5–68.5 ka) and the first half of Stadial D (7.30–6.84 m; ca. 73.5–68.5 ka), therefore covering the MIS 5/4 transition (Müller et al., 2003). The initial increases of *Sergentia coracina*-type and *Tanytarsus lugens*-type that began in CZF 2 continue, which in shallow water environment imply continued cooling (Frey, 1988; Brundin, 1949; Brooks et al., 2007; Heiri et al., 2011). *Paratanytarsus austriacus*-type also appears, lending further evidence to a cooling (Boggero et al., 2006; Brooks et al., 2007; Heiri et al., 2011). Littoral non-chironomid remains including oribatid mites and Sialidae decrease, possibly indicating a somewhat higher lake level. Towards the end of the zone during the Dürnten interstadial beginning at ca. 71 ka, increasing abundance of *Corynocera ambigua* with associated decreases in *Sergentia coracina*-type and *Tanytarsus lugens*-type and the removal of *Paratanytarsus austriacus*-type possibly imply warming.

CZF 4 (6.84–6.54 m; ca. 73.5–55 ka) represents the later part of Stadial D and is characterized by a large increase of *Corynocera oliveri*, a cold stenotherm taxon typical of cold arctic environments (Brooks and Birks, 2000), at the onset. *Sergentia coracina*-type and *Tanytarsus lugens*-type have been shown to dominate the chironomid assemblage under cold climatic conditions in shallow-water environments (Brooks et al., 2007; Frey, 1988; Heiri et al., 2011; Nazarova et al., 2017). Following CZF 4 there is a short interval (6.54–6.40 m; ca. 55–53 ka) in which chironomid head capsules and other aquatic invertebrate fossils decrease in abundance or were absent, suggesting that lake productivity may have been too low to maintain abundant and diverse chironomid assemblages, or that the lake shallowed and dried out at the coring site. A lake-drying interval is supported by peak abundances of *Smittia/Pseudosmittia,* that are indicative of shallow lakes, and Sciaridae (terrestrial midge) head capsules immediately following the 6.54–6.40 m core section.

CZF 5 (6.40–6.04 m; ca. 53–49 ka), corresponding to the Bellamont 1 interstadial (within MIS 3; Müller et al., 2003) consists of four samples. This zone displays relatively high abundances of *Tanytarsus mendax*-type, a chironomid morphotype typical of relatively warm temperatures (Brooks et al., 2007; Heiri et al., 2011), whereas many chironomids that were already dominant in the previous zones return at low abundances, confirming lacustrine conditions. Above 6.04 m core depth, the sediment contained <1 chironomid per cm^3, again suggesting that the lake may not have been productive enough to support abundant and diverse chironomid assemblages or that the lake shallowed and dried at the coring site.

In summary, chironomid assemblages in the Füramoos record indicate relatively shallow, near-shore environments over the entire analysed sediment section, which spans from ca. 99 to 49 to ka. Overall there is an increase along the sequence of chironomid taxa that are, in shallow-water environments, indicative of relatively cool climate conditions. Several relatively minor changes in chironomid assemblages and other invertebrate remains suggest moderate changes in lake level and lake depth at both FU1/FU3 and FURA coring sites. The absence of Chironomidae in high enough abundance and diversity to analyse between CZF 4 and CZF 5, as well as after CZF 5, is attributed to low lake productivity or a decrease of the lake level leaving the coring site dry.

4.2. Chironomid-inferred temperature and coeval Füramoos pollen data

Pollen evidence from Würmian sediments at Füramoos describes a series of stadial and interstadial conditions which can be seen as phases of forest opening and forest reestablishment and/or closing respectively (Fig. 2; Müller et al., 2003). The new chironomid record represents four interstadials, i.e., the late Brörup, Odderade, Dürnten and Bellamont 1, associated with increased arboreal pollen percentages relative to the adjacent stadials preceding and/or following them. The stadials (named Stadials B, C and D) have been correlated with climatic changes in the North Atlantic by Müller et al. (2003). In general, the arboreal taxa present at Füramoos over the study interval are *Pinus*, *Picea* and *Betula*. In addition, there are a series of thermophilous tree taxa for the earliest Würmian, and the stadials are associated with increased percentages of herbs such as Poaceae and *Artemisia* (Müller et al., 2003).

Chironomid-inferred temperatures ranged from 7.8 to 17.7 °C in the studied sediment section between ca. 99 and 49 ka. Many of the encountered chironomid assemblages have no close modern analogues in the modern calibration data (Fig. 4) and, in some parts of the section (beginning of Odderade and Dürnten) assemblages have a poor or very poor fit with temperature. However, WA-PLS regression usually performs relatively well in non-analogue situations (Lotter et al., 1999). The moderate lake-level changes

suggested by the ecological analyses of the chironomid and other invertebrate assemblages (see Section 4.1.) may have had some influence on the temperature reconstruction. However, lakes with a wide depth range are incorporated in the applied calibration dataset and transfer function (0.9–85 m water depth; Heiri and Lotter, 2010; Heiri et al., 2011), and the influence of water depth on the reconstruction is therefore incorporated in the prediction error of the model and the sample-specific estimated standard errors of prediction, which ranged from 1.4 to 1.7 °C. The strongest influence of past lake-level changes can be expected within the Bellamont 1 interstadial for a single sample, where very high abundances of semi-terrestrial chironomids (*Smittia/Pseudosmitta*) and terrestrial midge remains (Sciaridae) suggest very low water depth. This sample immediately follows the interval 6.54–6.40 m in which there were no chironomids found. XRF analysis in the section 6.41–6.39 m indicates an increase of S and Ca which could indicate an increase in evaporative minerals such as gypsum and calcite. This seems to corroborate the inference of decreasing lake level inferred by high abundances of *Smittia/Pseudosmitta*. There is also a persistent presence of the alga *Pediastrum* throughout the 6.54–6.40 m interval, which has been recorded in peat bogs, puddles and intermittent ponds (Moore, 1974; Komárek and Jankovská, 2001). Based on earlier studies of chironomid assemblages from lake surface sediments, such shallow water conditions may have led to an overestimation of July temperatures (Heiri et al., 2003a). However, inferred temperatures from this sample are not noticeably different from other Bellamont 1 interstadial samples.

The most pronounced short-term (centennial-scale) temperature variations are recorded for the Odderade interstadial (11.93–8.49 m; ca. 84.5–77 ka). Short-term (single-sample) maxima and minima are inferred in this section. However, the amplitude of these short-term variations exceeds expected variations in mean July temperature during the early Würmian. A more pronounced (3-sample) centennial-scale temperature decrease to ca. 8.5 °C is also apparent in the early part of the Odderade interstadial between 11.47 and 10.95 m (ca. 83–82 ka) that does not agree with reported stadials from Central Europe. These minimum temperatures are associated with >65% abundance of *Corynocera ambigua*, a species originally described as a cold indicator (Luoto, 2009a) and found to dominate relatively cool samples of the applied transfer function and calibration dataset (Heiri et al., 2011). However, several studies have shown that in some situations *C. ambigua* can occur in relatively warm climatic conditions, such as eutrophic lowland lakes in Denmark (Brodersen and Lindegaard, 1999) or relatively warm lakes in Russia (Nazarova et al., 2015). Hence, the temperature preference of this species is not clearly constrained by presently available ecological studies. Short-term temperature excursions in this part of the record should therefore be interpreted with caution unless further independent evidence becomes available for a centennial-scale temperature variation within the Odderade Interstadial.

4.2.1. Brörup interstadial (Br)

Sediments attributed to the Brörup interstadial (ca. 99–87 ka) are associated with chironomid-inferred July air temperatures of ca. 13.5–14.5 °C. Müller et al. (2003) indicate dominance of arboreal pollen representing cool temperate to boreal forests consisting primarily of *Pinus, Betula* and *Picea* for the same interval and therefore the new temperature reconstruction is in agreement with the pollen assemblage. During peak interstadial conditions, climate was favourable for the growth of thermophilous tree taxa such as *Carpinus*, *Quercus* and *Corylus*, which reached up to 15% (Müller et al., 2003). Although our new chironomid record does not cover the Brörup climatic optimum, it describes the late Brörup interval and transition into Stadial B, thereby providing a basis from which to analyse the climatic development of Stadial B.

4.2.2. Stadial B (SB)

Average chironomid-inferred July air temperatures during Stadial B (ca. 87–84.5 ka) at Füramoos were 13.7 °C, values slightly lower (<1 °C) than during the Brörup interstadial. The new pollen data show high *Artemisia* and low arboreal pollen in this interval (Fig. 2) supporting previous work by Müller et al. (2003). This suggests a forest opening during the Stadial B interval. The organic-matter content in the sediments also decreases, and higher *Artemisia* percentages document an increase in steppe conditions and a dryer climate (Müller et al., 2003). The absence of major chironomid-inferred temperature change during Stadial B suggests that summer-temperature changes are unlikely to have resulted in the observed vegetation turnover and forest opening. Previous work by Lotter et al. (2012) suggests that chironomids and vegetation respond differently to seasonal temperature and humidity changes, with chironomids being more influenced by summer temperature and vegetation being more influenced by winter temperature and precipitation. Therefore, it appears that either changes in winter temperature, continentality or moisture availability drove forest opening during Stadial B.

4.2.3. Odderade (Odd)

The early part of the Odderade interstadial (ca. 84.5–77 ka) is characterised by an increase in chironomid-inferred July air temperatures from 14 °C to slightly higher values, with a single-sample peak of 17.7 °C. Pollen assemblages in this part of the record almost reach 100% arboreal pollen (Fig. 2) and Müller et al. (2003) show that different thermophilous tree taxa such as *Quercus*, *Corylus* and *Carpinus* were abundant at the very beginning of the Odderade, present at pollen abundances >20%. Chironomid-inferred temperatures from Füramoos are very variable in this part of the record, and as discussed above, short-term inferred cooling in this section (ca. 83–82 ka) should be interpreted with caution. Most of the early Odderade represents a “no-good” modern-analogue situation and contains samples with a “poor” goodness of fit to temperature (Fig. 4). The later cooling into Stadial C is associated with generally improved fit to temperature statistics and samples that have closer modern analogues (Fig. 4). Overall, we observe a general, long-term decrease in chironomid-inferred temperatures from the onset to the end of the Odderade, falling from initial temperatures of ca. 15 °C to as low as 11 °C. This cooling is associated with a decline in tree-pollen percentages over the Odderade interstadial interval (Fig. 5).

4.2.4. Stadial C (SC)

July temperature reconstructions for Stadial C (ca. 77–74.5 ka) range from 7.8 to 11 °C (Fig. 4), with a sustained interval of ca. 9 °C. These temperatures are typical for treeline or low-tundra environments in Central Europe (Landolt, 2003). In accordance, tree-pollen percentages abruptly decrease at Füramoos during Stadial C (Fig. 2), with an almost complete disappearance of both *Pinus* and *Picea* pollen at the onset of Stadial C, *Betula* contributing the majority of the arboreal pollen and *Artemisia* increasing in the pollen record (Müller et al., 2003). Tree *Betula* has not been differentiated from the shrub birch *Betula nana* in this interval so it is possible that either tree *Betula* survived in isolated stands during Stadial C or that summer temperatures became too cool to sustain tree growth.

4.2.5. Dürnten (Du)

Sediments correlated to the Dürnten interstadial (ca. 74.5–68.5 ka) are associated with a chironomid-inferred July temperature increase to 10 °C (Fig. 4). During this interval the local pollen assemblage shows a decrease in *Artemisia* percentages and an

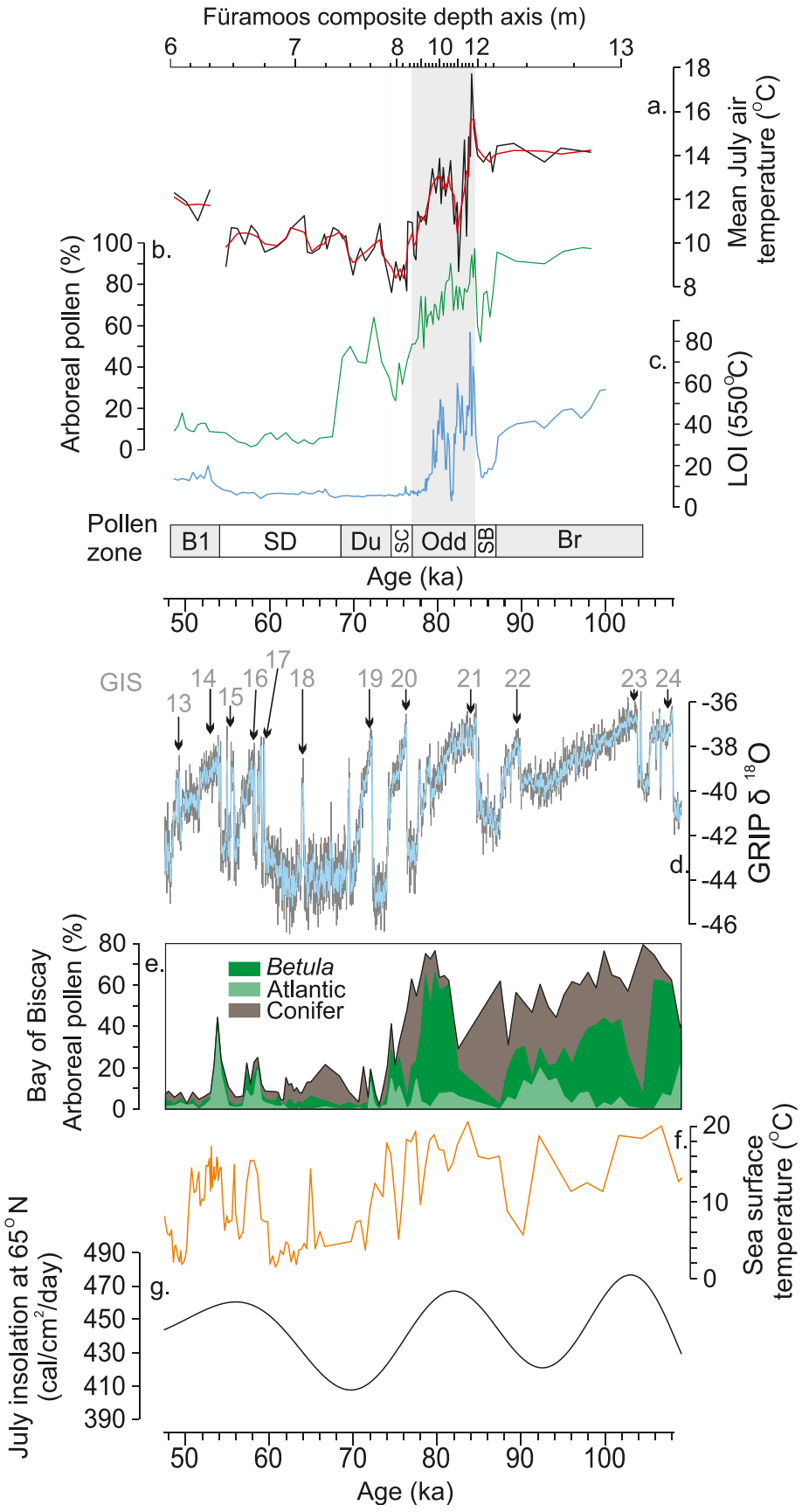

Fig. 5. a. Chironomid-inferred July air temperature reconstruction (black) and three sample running average (red); b. Füramoos composite core arboreal pollen percentages; c. Füramoos composite core LOI at 550 °C; d. NGRIP $\delta^{18}O$ record, Greenland (North Greenland Ice Core Project members 2004). Greenland Isotope Stages (GIS) are indicated (Rasmussen et al., 2014); e: Bay of Biscay (core MD04-2845) pollen record. Atlantic forest pollen includes *Corylus, Carpinus, Fagus*, deciduous *Quercus* and *Betula* (*Betula* presented separately; Sánchez Goñi et al., 2008, 2013); f. June, July, August sea-surface temperatures from the Bay of Biscay (core MD04-2845) (Sánchez Goñi et al., 2008); g. Summer insolation at 65°N (Berger and Loutre, 1991). MD04-2845 data presented on ACER project members (2017) chronology. (For interpretation of the references to colour in this figure legend, the reader is referred to the Web version of this article.)

increase in arboreal pollen indicating forest expansion at Füramoos (Fig. 2). As trees require summer temperatures exceeding 8.5–10 °C to grow depending on the species (Landolt, 2003), this finding is in agreement with the chironomid-based temperature record.

4.2.6. Stadial D (SD)

Chironomid-inferred temperatures during Stadial D remain at 9.5–10.5 °C (three sample running average; Fig. 5), while arboreal pollen is reduced to 20% and *Artemisia* expands, suggesting the development of an arctic tundra or steppe environment. Previously, Müller et al. (2003) suggested that the cooling associated with the beginning of Stadial D eliminated local refugia and prevented remigration of tree taxa through the Stadial D interval. Based on size measurements of pollen grains, these authors showed that *Betula* largely originated from the dwarf shrub *Betula nana*, leading them to conclude that most areas north of the Alps were completely treeless during this interval. Our new chironomid-inferred temperatures support this hypothesis. Fluctuating around 10 °C July temperature, they are at upper limit of the reported minimum temperature requirement for tree growth in Central Europe (Landolt, 2003).

4.2.7. Bellamont 1 (B1)

For Bellamont 1, chironomid-inferred July temperatures show an increase from 9.5 to 10.5 °C to ca. 12 °C based on three sample running averages (Fig. 5). Earlier pollen analyses at Füramoos showed that this interval was characterized by the immigration of plants typical for a slightly warmer climate than during Stadial D, such as *Juniperus*, *Hippophaë* and *Selaginella*, and analyses of *Betula* pollen suggest the re-imigration of the tree birch *Betula alba* (Müller et al., 2003). The increase in tree-pollen percentages is corroborated by our own pollen data (Fig. 5) leading us to conclude that more favourable summer temperatures above 10 °C (Landolt, 2003) facilitated tree remigration to the Füramoos site.

4.3. Comparison with other quantitative summer temperature estimates from Europe

There are few quantitative palaeotemperature records from central and western Europe that cover large parts of the examined interval and can be directly compared with our chironomid-based temperature reconstruction, mainly based on pollen and beetle (coleopteran) records. In the following discussion we use the correlations between previously published European temperature records and our Füramoos dataset as outlined in Supplementary Information 1. For the earliest part of our record, absolute July air temperature values reconstructed based on other approaches generally agree with our new chironomid-based temperature reconstruction. For example, Brörup July temperature ranges produced from our new chironomid record (13.5–14.5 °C) fall within the temperature ranges yielded by beetle assemblages at Gröbern (range of reconstructed temperature ranges of 12–17 °C; Walkling and Coope, 1996), Oerel (11–19 °C; Behre et al., 2005) and La Grande Pile (9–26 °C; Ponel, 1995) as well as the available pollen reconstructions from Füramoos, Jammertal, Les Echets, Samerberg (Klotz et al., 2004) and Gröbern (Kühl et al., 2007; range of reconstructed means: 9.5–20 °C; Supplementary Table 1). Interestingly, neither the temperature ranges presented from these records nor our new chironomid-based record suggest major summer-temperature cooling during Stadial B, with only the lowermost estimated temperature range of the Gröbern beetle record (9–16 °C for Stadial B; Walkling and Coope, 1996) falling below 10 °C. This may suggest that summer temperature did not play a major role in forest opening during this interval. For the interval from Stadial D to the Bellamont 1 interstadial, the only summer-temperature records available for comparison are from La Grande Pile (Ponel, 1995) and Oerel (Behre et al., 2005), both of which are based on beetle remains. All three available temperature records (i.e., Füramoos – this study; Oerel – Behre et al., 2005; La Grande Pile – Ponel, 1995) suggest that MIS 3 interstadial summer temperatures were colder than during MIS 5c and MIS 5a, with the exception of the upper temperature range reconstructed from La Grande Pile following the Pile complex (21 °C; see Supplementary Table 1). This range of 9.5–13.5 °C suggests that summer temperatures during the MIS 3 interstadials were cool, but still warm enough in the interstadial sections to support the growth of trees that can survive at the transition zone from tundra to forest in Central Europe. This scenario is corroborated by the Füramoos pollen record, which shows an increase in the percentages of arboreal pollen, primarily of the pioneer *Betula,* in the Bellamont 1 interglacial (Müller et al., 2003).

4.4. Comparison with Atlantic and European palaeoclimate records

Our chironomid-based temperature record indicates a pronounced, long-term decrease in July temperatures in Central Europe, from values around 14 °C in the Brörup interstadial to values around 8.5 °C in Stadial C (Fig. 5), with minimum temperatures in this stadial. The mean temperature of the warmest month as inferred through beetle-based reconstructions from La Grande Pile, France (Ponel, 1995; Guiter et al., 2003), also shows a transition to cooler temperatures across this interval, as do pollen-based reconstructions of mean annual temperature at Les Echets and La Grande Pile (Guiot et al., 1993). Conspicuous declines in tree pollen abundances are observed across the interval at Füramoos (Müller et al., 2003) and many other terrestrial European sites (e.g. Jammertal: Müller, 2000; Samerberg: Grüger, 1979; La Grande Pile: Woillard, 1978; Oerel: Behre and Lade, 1986). Similar vegetational transitions are documented in pollen records from the Iberian margin and the North Atlantic, with more thermophilic assemblages transitioning to less thermophilic assemblages (Sánchez Goñi et al., 2008). Furthermore, there is a general increase in the cold-indicating planktonic foraminifer *N. pachyderma* (s) at these locations, although the long-term trend is strongly influenced by short-term variations on the centennial-scale for this species within the examined sediment records (Sánchez Goñi et al., 2008). Our new chironomid record from Füramoos agrees with these reconstructed trends towards cooler temperatures, although the decrease in chironomid-inferred temperatures appears to happen earlier (ca. 85–75 ka) than in the Iberian and North Atlantic records (ca. 80–70 ka). This millennial-scale temperature decrease in the Füramoos chironomid record occurs together with a pronounced decrease in Northern Hemisphere summer insolation (Berger and Loutre, 1991, Fig. 5), indicating that summer temperatures in this interval may have been strongly affected by insolation changes. It also suggests that the transition of vegetation types reconstructed for Füramoos based on pollen (Müller et al., 2003) may have been driven to a considerable extent by decreasing summer temperatures, particularly for younger sections of this interval (Fig. 5). Whereas July air temperatures around 14 °C as recorded for earlier parts of the record may sustain a wide range of European tree taxa and forest types, temperatures around 8.5–11 °C as inferred for the youngest sections (Stadial C to Stadial D) can only be tolerated by boreal and subalpine trees such as *Betula*, *Picea* or *Pinus*. These temperature values are typical for the transition between forest and tundra in Central Europe (Landolt et al., 2003).

It has been shown that climatic conditions in Europe during the Würmian glaciation covaried with centennial-scale variations in North Atlantic climate and ocean circulation. Greenland ice core $\delta^{18}O$ records indicate a series of stadials and interstadials also

observed in variations in speleothem $\delta^{18}O$ records from Central Europe (Boch et al., 2011). There were also centennial-scale decreases in polar foraminifera in the North Atlantic (McManus et al., 1994; Sánchez Goñi et al., 2008) and, for interstadials during the early Würmian, there were expansions of more thermophilous tree taxa in continental Europe (Müller, 2000, Müller et al., 2003; Sánchez Goñi et al., 2008; Wulf et al., 2018, Fig. 5). Pollen records from the Iberian margin suggest variable, but decreasing temperatures in the interval covered by our record (Sánchez Goñi et al., 2008; Fletcher et al., 2010). As indicated above, the most pronounced millennial-scale cooling as recorded by pollen assemblages in the Bay of Biscay appeared to have been between ca. 80–70 ka. However, this longer-term trend was interrupted by shorter term, pollen inferred intervals of warmer climate that have been correlated with GIS 21–19 (Sánchez Goñi et al., 2008). Similarly, vegetation changes associated with the Odderade and Dürnten interstadials, that have been correlated with GIS 20 and 21, have been observed in the pollen record of Füramoos (Müller et al., 2003, Fig. 5). The new chironomid-based July air temperature reconstruction shows some evidence of minor temperature increases at the onset of the Odderade and Dürnten interstadials (Müller et al., 2003). However, overall centennial-scale temperature variations that could be related to stadial-interstadial transitions are not very pronounced and less prominent than the multi-millennial-scale temperature trends in the data.

During Stadial D, regions north of the Alps are considered to have been largely treeless, with most local tree refugia eradicated (Müller et al., 2003). Based on the correlation of the Füramoos record with the Greenland isotope records by Müller et al. (2003), GIS stages 19, 18 and 17 occurred during the Stadial D interval. However, short term variations in pollen assemblages during Stadial D that could represent vegetation change during GIS 19–17 are not detected in the Füramoos record (Müller et al., 2003, Fig. 5). Since particularly GIS 19–18 were relatively short-lived events (Fig. 5), it is possible that this is a matter of sample resolution. However, there are other examples of pollen records from Europe in which one or more of the GIS stages 19, 18 and 17 are absent (Fletcher et al., 2010). Chironomid-inferred July air temperatures for Stadial D vary between 9 and 10.5 °C and also present no clear indication of GIS stages 19, 18 and 17. Overall our results suggest that July air temperature appears to have played an important role in driving vegetation change during some sections of the Füramoos record, particularly during the inferred temperature decrease and temperature minimum during the Odderade and Stadial C (Fig. 5). However, in other intervals summer temperature was apparently not limiting tree growth or driving vegetation change. For example, the chironomid inferred July air temperatures for Stadial D are typical for treeline or low-tundra environments in Central Europe (Landolt, 2003). If local arboreal refugia would have been present, increases in arboreal pollen associated with temperatures above 10 °C would have been expected assuming the other taxa specific demands for tree growth had been met, however no such arboreal pollen increase is observed. Similarly, during Stadial B, arboreal pollen decreases from 95 to 50%, while reconstructed July air temperature decreases only 0.5 °C, remaining at similar values as during parts of the Brörup. This implies that summer temperature change was not the driver of this forest opening in the Füramoos region. The latter observation agrees with the review of Helmens (2014) who reports very little summer temperature change in Europe during MIS 5b relative to MIS5c and MIS5a, the intervals corresponding to the Brörup-Stadial B-Odderade transitions.

5. Conclusions

We present the longest chironomid-based, quantitative temperature reconstruction from the Würmian glacial period to date, covering the interval from the Brörup (MIS 5c; ca. 99 ka) to the Bellamont 1 interstadials (MIS 3; ca. 49 ka) at centennial to millennial resolution. Chironomid assemblages suggest that the study site at Füramoos was a relatively shallow lake during this interval, with assemblages indicating warmer conditions (dominated, e.g., by *Cladopelma lateralis*-type, *Tanytarsus mendax*-type, *Microtendipes pedellus*-type and *Dicrotendipes nervosus*-type) over the course of the record giving way to assemblages indicating cooler conditions (dominated, e.g., by *Tanytarsus lugens*-type and *Sergentia coracina*-type). Both the chironomid assemblages and associated non-chironomid remains suggest that during the interval ca. 55–53 ka and following ca. 49 ka, the lake either shallowed and dried out at the coring site, or was not productive enough to support abundant and diverse invertebrate assemblages.

The chironomid-based July temperature reconstruction shows decreasing temperatures of ca. 14 °C in the Brörup, ca. 14 °C during Stadial B, 10–16 °C during the Odderade, 9 °C during Stadial C, 10–11 °C during the Dürnten and Stadial D, and an increase to 12 °C during the Bellamont 1 interstadial. Overall, our results support other palaeotemperature records from Europe in indicating a distinct cooling during the early to middle Würmian. The strongest summer temperature decrease is registered in our record during the Odderade interstadial, synchronous with a major decrease in summer insolation and prior to forest opening and development of a steppic tundra associated with MIS 4. The inferred summer-temperature decrease during Stadial B was relatively minor, and inferred temperatures during Stadial D were cool but variable. The lowest summer temperatures in the examined interval prevailed during Stadial C, with initial July air temperature decreases beginning during the Odderade interstadial when cool summers may have contributed to the elimination of forests at Füramoos and wider Central Europe.

Declaration of competing interest

The authors declare that they have no known competing financial interests or personal relationships that could have appeared to influence the work reported in this paper.

Acknowledgements

The contributions of Bertil Mächtle and Gerd Schukraft (†) to the FU1/FU3 coring campaign, and of George Kukla (†), Ulrich Müller and Guy Seret to the FURA coring campaign are gratefully acknowledged. We also thank Nichole Anest for core handling at the Lamont-Doherty Core Repository. We thank both reviewers for helpful suggestions that have improved our manuscript. This research has been supported by the Swiss National Science Foundation (SNSF grant 200021_165494).

Author statement

Alexander Bolland: Conceptualization, Methodology, Validation, Formal analysis, Writing – original draft Project administration, Investigation, Data curation Visualization Resources Writing – review & editing. Oliver Heiri: Conceptualization, Methodology, Validation, Formal analysis, Writing – original draft Project administration, Supervision, Resources Writing – review & editing.

Funding acquisition. Supervision. Oliver Kernt: Investigation. Resources Writing – review & editing. Frederik Allstädt: Investigation. Andreas Koutsodendris, Resources Writing – review & editing. Supervision. Jörg Pross, Resources Writing – review & editing. Supervision. Dorothy Peteet: Resources Writing – review & editing.

Data availability

Chironomid data associated with this study as well as the chironomid-inferred temperature data have been deposited at the Dryad online data repository: https://doi.org/10.5061/dryad.dfn2z351t (www.datadryad.org/).

Appendix A. Supplementary data

Supplementary data to this article can be found online at https://doi.org/10.1016/j.quascirev.2021.107008.

References

ACER project members, 2017. CLAM Age Model and Biomes of Sediment Core MD04-2845. PANGAEA. https://doi.org/10.1594/PANGAEA.872808.

Chironomidae of the holarctic region: keys and diagnoses: larvae. In: Andersen, T., Cranston, P.S., Epler, J.H. (Eds.), 2013. Scandinavian Society of Entomology.

Beattie, D.M., 1982. Distribution and production of the larval chironomid populations in Tjeukemeer. Hydrobiologia 95 (1), 287–306.

de Beaulieu, J.L.D., Reille, M., 1984. A long upper Pleistocene pollen record from Les Echets, near Lyon, France. Boreas 13 (2), 111–132.

de Beaulieu, J.L., Reille, M., 1989. The transition from temperate phases to stadials in the long Upper Pleistocene sequence from Les Echets (France). Palaeogeogr. Palaeoclimatol. Palaeoecol. 72, 147–159.

Behre, K.E., 1989. Biostratigraphy of the last glacial period in Europe. Quat. Sci. Rev. 8 (1), 25–44.

Behre, K.E., Lade, U., 1986. Eine Folge von Eem und 4 Weichsel-Interstadialen in Oerel/Niedersachsen und ihr Vegetationsablauf. E&G Quaternary Science Journal 36 (1), 11–36.

Behre, K.E., van der Plicht, J., 1992. Towards an absolute chronology for the last glacial period in Europe: radiocarbon dates from Oerel, northern Germany. Veg. Hist. Archaeobotany 1 (2), 111–117.

Behre, K.E., Hölzer, A., Lemdahl, G., 2005. Botanical macro-remains and insects from the Eemian and Weichselian site of Oerel (northwest Germany) and their evidence for the history of climate. Veg. Hist. Archaeobotany 14 (1), 31–53.

Bennett, K.D., 1996. Determination of the number of zones in a biostratigraphical sequence. New Phytol. 132 (1), 155–170.

Berger, A., Loutre, M.F., 1991. Insolation values for the climate of the last 10 million years. Quat. Sci. Rev. 10 (4), 297–317.

Beug, H.J., 2004. Leitfaden der Pollenbestimmung für Mitteleuropa und angrenzende Gebiete. Dr. Friedrich Pfeil, München.

Birks, H.J.B., Braak, C.T., Line, J.M., Juggins, S., Stevenson, A.C., 1990. Diatoms and pH reconstruction. Philos. Trans. R. Soc. Lond. B Biol. Sci. 327 (1240), 263–278.

Boch, R., Cheng, H., Spötl, C., Edwards, R.L., Wang, X., Häuselmann, Ph, 2011. NALPS: a precisely dated European climate record 120–60 ka. Clim. Past 7 (4), 1247–1259.

Boggero, A., Füreder, L., Lencioni, V., Simcic, T., Thaler, B., Ferrarese, U., Lotter, A.F., Ettinger, R., 2006. Littoral chironomid communities of Alpine lakes in relation to environmental factors. Hydrobiologia 562 (1), 145–165.

Bolland, A., Rey, F., Gobet, E., Tinner, W., Heiri, O., 2020. Summer temperature development 18,000–14,000 cal. BP recorded by a new chironomid record from Burgäschisee, Swiss Plateau. Quat. Sci. Rev. 243, 106–484.

ter Braak, C.J., Juggins, S., 1993. Weighted averaging partial least squares regression (WA-PLS): an improved method for reconstructing environmental variables from species assemblages. Twelfth International Diatom Symposium. Springer, Dordrecht, pp. 485–502.

ter Braak, C.J.F., Juggins, S., Birks, H.J.B., van der Voet, H., 1993. Weighted averaging partial least squares regression (WA-PLS): definition and comparison with other methods for species-environment calibration. In: Patil, G.P., Rao, C.R. (Eds.), Multivariate Environmental Statistics. Elsevier Science Publishers B.V., Amsterdam, pp. 525–560.

ter Braak, C.J., Smilauer, P., 2018. Canoco Reference Manual and User's Guide: Software for Ordination (Version 5.10). Wageningen University & Research, Biometris.

Brodersen, K.P., Lindegaard, C., 1999. Mass occurrence and sporadic distribution of Corynocera ambigua Zetterstedt (Diptera, Chironomidae) in Danish lakes. Neo- and palaeolimnological records. J. Paleolimnol. 22 (1), 41–52.

Brooks, S.J., Birks, H.J.B., 2000. Chironomid-inferred late-glacial and early-Holocene mean July air temperatures for Kråkenes Lake, western Norway. J. Paleolimnol. 23 (1), 77–89.

Brooks, S.J., Langdon, P.G., Heiri, O., 2007. The identification and use of Palaearctic Chironomidae larvae in palaeoecology. Quaternary Research Association Technical Guide 10, 1–275.

Brundin, L., 1949. Chironomiden und ander Bodentiere de sudschwedischen Urgebirgseen. Ein Beitrag zur Kenntnis der bodenfaunistischen Charakterzuge schwedischer oligotropher Seen, vol. 30. Report of the Insitute of Freshwater Research, Drottningholm, pp. 1–914.

Busschers, F.S., Van Balen, R.T., Cohen, K.M., Kasse, C., Weerts, H.J., Wallinga, J., Bunnik, F.P., 2008. Response of the Rhine–Meuse fluvial system to Saalian ice-sheet dynamics. Boreas 37 (3), 377–398.

Caspers, G., Freund, H., 2001. Vegetation and climate in the early-and pleniweichselian in northern central Europe. J. Quat. Sci.: Published for the Quaternary Research Association 16 (1), 31–48.

Chaline, J., Jerz, H., 1984. Arbeitsergebnisse der Subkommission für Europäische Quartärstratigraphie. Stratotypen des Würm-Glazials. Eiszeitalt. Ggw. 35, 185–206.

de la Riva-Caballero, A., Birks, H.J.B., Bjune, A.E., Birks, H.H., Solhøy, T., 2010. Oribatid mite assemblages across the tree-line in western Norway and their representation in lake sediments. J. Paleolimnol. 44 (1), 361–374.

Dansgaard, W., Johnsen, S.J., Clausen, H.B., Dahl-Jensen, D., Gundestrup, N.S., Hammer, C.U., Hvidberg, C.S., Steffensen, J.P., Sveinbjörnsdottir, A.E., Jouzel, J., Bond, G., 1993. Evidence for general instability of past climate from a 250-kyr ice-core record. Nature 364 (6434), 218–220.

DWD Climate Data Center (CDC), 2021. Historische monatliche Stationsbeobachtungen (Temperatur, Druck, Niederschlag, Sonnenscheindauer, etc.) für Deutschland, 3.

Eggermont, H., Heiri, O., 2012. The chironomid-temperature relationship: expression in nature and palaeoenvironmental implications. Biol. Rev. 87 (2), 430–456.

Eisele, G., Haas, K., Liner, S., 1994. Methode zur Aufbereitung fossilen Pollens aus minerogenen Sedimenten. In: Frenzel, B. (Ed.), Über Probleme der holozänen Vegetationsgeschichte Osttibets, vol. 95. Göttingen, Göttinger Geographische Abhandlungen, pp. 165–166.

Engels, S., Bohncke, S.J., Heiri, O., Schaber, K., Sirocko, F., 2008. The lacustrine sediment record of Oberwinkler Maar (Eifel, Germany): chironomid and macroremain-based inferences of environmental changes during Oxygen Isotope Stage 3. Boreas 37 (3), 414–425.

Engels, S., Helmens, K.F., Väliranta, M., Brooks, S.J., Birks, H.J.B., 2010. Early Weichselian (MIS 5d and 5c) temperatures and environmental changes in northern Fennoscandia as recorded by chironomids and macroremains at Sokli, northeast Finland. Boreas 39 (4), 689–704.

Engels, S., Self, A.E., Luoto, T.P., Brooks, S.J., Helmens, K.F., 2014. A comparison of three Eurasian chironomid–climate calibration datasets on a W–E continentality gradient and the implications for quantitative temperature reconstructions. J. Paleolimnol. 51 (4), 529–547.

Fletcher, W.J., Goni, M.F.S., Allen, J.R., Cheddadi, R., Combourieu-Nebout, N., Huntley, B., Lawson, I., Londeix, L., Magri, D., Margari, V., Müller, U.C., 2010. Millennial-scale variability during the last glacial in vegetation records from Europe. Quat. Sci. Rev. 29 (21–22), 2839–2864.

Fjellberg, A., 1972. Present and late weichselian occurrence of Corynocera ambigua zett. (Diptera, Chironomidae) in Norway. Norweg. J. Entomol. 19 (1972), 59–61.

Francis, D.R., 2001. Bryozoan statoblasts. In: Smol, J.P., Birks, H.J.B., Last, W.M. (Eds.), Tracking Environmental Change Using Lake Sediments Volume 4 Zoological Indicators, vol. 4. Kluwer Academic Publishers, Dordrecht, pp. 105–123.

Frey, D.G., 1988. Littoral and offshore communities of diatoms, cladocerans and dipterous larvae, and their interpretation in paleolimnology. J. Paleolimnol. 1 (3), 179–191.

Gandouin, E., Rioual, P., Pailles, C., Brooks, S.J., Ponel, P., Guiter, F., Djamali, M., Andrieu-Ponel, V., Birks, H.J.B., Leydet, M., Belkacem, D., 2016. Environmental and climate reconstruction of the late-glacial-Holocene transition from a lake sediment sequence in Aubrac, French Massif Central: chironomid and diatom evidence. Palaeogeogr. Palaeoclimatol. Palaeoecol. 461, 292–309.

Grimm, E.C., 1987. CONISS: a Fortran 77 program for stratigraphically constrained cluster analysis by the method of incremental sum of squares. Comput. Geosci. 13 (1), 13–35.

Grüger, E., 1979. Spätriss, Riss/Würm und Frühwürm am Samerberg in Oberbayern—ein vegetationsgeschichtlicher Beitrag zur Gliederung des Jungpleistozäns. Geol. Bavarica 80, 5–64.

Guiot, J., De Beaulieu, J.L., Cheddadi, R., David, F., Ponel, P., Reille, M., 1993. The climate in Western Europe during the last Glacial/Interglacial cycle derived from pollen and insect remains. Palaeogeogr. Palaeoclimatol. Palaeoecol. 103 (1), 73–93.

Guiter, F., Andrieu-Ponel, V., de Beaulieu, J.L., Cheddadi, R., Calvez, M., Ponel, P., Reille, M., Keller, T., Goeury, C., 2003. The last climatic cycles in Western Europe: a comparison between long continuous lacustrine sequences from France and other terrestrial records. Quat. Int. 111 (1), 59–74.

Haas, J.N., 1994. First identification key for charophyte oospores from central Europe. Eur. J. Phycol. 29 (4), 227–235.

Heggen, M.P., Birks, H.H., Heiri, O., Grytnes, J.A., Birks, H.J.B., 2012. Are fossil assemblages in a single sediment core from a small lake representative of total deposition of mite, chironomid, and plant macrofossil remains? J. Paleolimnol. 48 (4), 669–691.

Heiri, O., 2004. Within-lake variability of subfossil chironomid assemblages in shallow Norwegian lakes. J. Paleolimnol. 32 (1), 67–84.

Heiri, O., Lotter, A.F., 2001. Effect of low count sums on quantitative environmental reconstructions: an example using subfossil chironomids. J. Paleolimnol. 26 (3), 343–350.

Heiri, O., Lotter, A.F., 2005. Holocene and Lateglacial summer temperature reconstruction in the Swiss Alps based on fossil assemblages of aquatic organisms: a review. Boreas 34 (4), 506–516.
Heiri, O., Lotter, A.F., 2007. Sciaridae in lake sediments: indicators of catchment and stream contribution to fossil insect assemblages. J. Paleolimnol. 38 (2), 183–189.
Heiri, O., Lotter, A.F., 2010. How does taxonomic resolution affect chironomid-based temperature reconstruction? J. Paleolimnol. 44 (2), 589–601.
Heiri, O., Millet, L., 2005. Reconstruction of late glacial summer temperatures from chironomid assemblages in lac lautrey (jura, France). J. Quat. Sci. 20 (1), 33–44.
Heiri, O., Lotter, A.F., Lemcke, G., 2001. Loss on ignition as a method for estimating organic and carbonate content in sediments: reproducibility and comparability of results. J. Paleolimnol. 25 (1), 101–110.
Heiri, O., Birks, H.J.B., Brooks, S.J., Velle, G., Willassen, E., 2003a. Effects of within-lake variability of fossil assemblages on quantitative chironomid-inferred temperature reconstruction. Palaeogeogr. Palaeoclimatol. Palaeoecol. 199 (1–2), 95–106.
Heiri, O., Lotter, A.F., Hausmann, S., Kienast, F., 2003b. A chironomid-based Holocene summer air temperature reconstruction from the Swiss Alps. Holocene 13 (4), 477–484.
Heiri, O., Brooks, S.J., Birks, H.J.B., Lotter, A.F., 2011a. A 274-lake calibration data-set and inference model for chironomid-based summer air temperature reconstruction in Europe. Quat. Sci. Rev. 30 (23–24), 3445–3456.
Heiri, O., Brooks, S.J., Renssen, H., Bedford, A., Hazekamp, M., Ilyashuk, B., Jeffers, E.S., Lang, B., Kirilova, E., Kuiper, S., Millet, L., Samartin, S., Toth, M., Verbruggen, F., Watson, J.E., Asch, N., Lammertsma, E., Amon, L., Birks, H.H., Birks, H.J.B., Mortensen, M.F., Hoek, W.Z., Magyari, E., Sobrino, C.M., Seppä, H., Tinner, W., Tonkov, S., Veski, S., Lotter, A.F., 2014. Validation of climate model-inferred regional temperature change for late-glacial Europe. Nat. Commun. 5, 4914.
Helmens, K.F., Risberg, J., Jansson, K.N., Weckström, J., Berntsson, A., Tillman, P.K., Johansson, P.W., Wastegård, S., 2009. Early MIS 3 glacial lake evolution, ice-marginal retreat pattern and climate at Sokli (northeastern Fennoscandia). Quat. Sci. Rev. 28 (19–20), 1880–1894.
Helmens, K.F., Väliranta, M., Engels, S., Shala, S., 2012. Large shifts in vegetation and climate during the Early Weichselian (MIS 5d-c) inferred from multi-proxy evidence at Sokli (northern Finland). Quat. Sci. Rev. 41, 22–38.
Helmens, K.F., 2014. The Last Interglacial–Glacial cycle (MIS 5–2) re-examined based on long proxy records from central and northern Europe. Quat. Sci. Rev. 86, 115–143.
Hofmann, W., 1983a. Stratigraphy of subfossil Chironomidae and Ceratopogonidae (insecta: Diptera) in late glacial littoral sediments from lobsigensee (Swiss plateau). Studies in the late quaternary of lobsigensee 4. Rev. Paléobiol. 2 (2), 205–209.
Hofmann, W., 1983b. Stratigraphy of cladocera and Chironomidae in a core from a shallow north German lake. Hydrobiologia 103 (1), 235–239.
Hofmann, W., 2001. Late-Glacial/Holocene succession of the chironomid and cladoceran fauna of the Soppensee (Central Switzerland). J. Paleolimnol. 25 (4), 411–420.
Hubbard, A., Sugden, D., Dugmore, A., Norddahl, H., Pétursson, H.G., 2006. A modelling insight into the Icelandic Last Glacial Maximum ice sheet. Quat. Sci. Rev. 25 (17–18), 2283–2296.
Hughes, P.D., Gibbard, P.L., Ehlers, J., 2013. Timing of glaciation during the last glacial cycle: evaluating the concept of a global 'Last Glacial Maximum' (LGM). Earth Sci. Rev. 125, 171–198.
Hughes, P.D., Gibbard, P.L., 2018. Global glacier dynamics during 100 ka Pleistocene glacial cycles. Quat. Res. 90 (1), 222–243.
Ilyashuk, E.A., Ilyashuk, B.P., Hammarlund, D., Larocque, I., 2005. Holocene climatic and environmental changes inferred from midge records (Diptera: Chironomidae, Chaoboridae, Ceratopogonidae) at Lake Berkut, southern Kola Peninsula, Russia. Holocene 15 (6), 897–914.
Ilyashuk, E.A., Ilyashuk, B.P., Heiri, O., Spötl, C., 2020. Summer temperatures and lake development during the MIS 5a interstadial: new data from the Unterangerberg palaeolake in the Eastern Alps, Austria. Palaeogeogr. Palaeoclimatol. Palaeoecol. 560, 110020.
Imbrie, J., Hays, J.D., Martinson, D.G., McIntyre, A., Mix, A.C., Morley, J.J., Pisias, N.G., Prell, W.L., Shackleton, N.J., 1984. In: Berger, A.L., et al. (Eds.), "The Orbital Theory of Pleistocene Climate: Support from a Revised Chronology of the Marine d18O Record" in Milankovitch and Climate Part 1. D. Reidel, pp. 269–305.
Ivy-Ochs, S., Kerschner, H., Reuther, A., Preusser, F., Heine, K., Maisch, M., Kubik, P.W., Schlüchter, C., 2008. Chronology of the last glacial cycle in the European Alps. J. Quat. Sci.: Published for the Quaternary Research Association 23 (6-7), 559–573.
Juggins, S., 2007. C2: Software for Ecological and Palaeoecological Data Analysis and Visualisation (User Guide Version 1.5). Newcastle University, Newcastle upon Tyne, p. 77.
Juggins, S., 2017. Rioja: Analysis of Quaternary Science Data, R Package Version, 0.9-21. http://cran.r-project.org/package=rioja.
Kern, O.A., Koutsodendris, A., Mächtle, B., Christanis, K., Schukraft, G., Scholz, C., Kotthoff, U., Pross, J., 2019. XRF core scanning yields reliable semiquantitative data on the elemental composition of highly organic-rich sediments: evidence from the Füramoos peat bog (Southern Germany). Sci. Total Environ. 697, 134110.
Klotz, S., Müller, U., Mosbrugger, V., de Beaulieu, J.L., Reille, M., 2004. Eemian to early Würmian climate dynamics: history and pattern of changes in Central Europe. Palaeogeogr. Palaeoclimatol. Palaeoecol. 211 (1–2), 107–126.
Komárek, J., Jankovská, V., 2001. Review of the green algae genus Pediastrum; Implication for pollenanalytical research. In: Bibliotheca Phycologica, vol. 108. Cramer J, Berlin-Stuttgart.
Korhola, A., Olander, H., Blom, T., 2000. Cladoceran and chironomid assemblages as qualitative indicators of water depth in subarctic Fennoscandian lakes. J. Paleolimnol. 24 (1), 43–54.
Kühl, N., Litt, T., Schölzel, C., Hense, A., 2007. Eemian and Early Weichselian temperature and precipitation variability in northern Germany. Quat. Sci. Rev. 26 (25–28), 3311–3317.
Landolt, E., 2003. Unsere Alpenflora. Gustav Fisher, Stuttgart, Germany.
Langdon, P.G., Ruiz, Z.O.E., Brodersen, K.P., Foster, I.D., 2006. Assessing lake eutrophication using chironomids: understanding the nature of community response in different lake types. Freshw. Biol. 51 (3), 562–577.
Langdon, P.G., Holmes, N., Caseldine, C.J., 2008. Environmental controls on modern chironomid faunas from NW Iceland and implications for reconstructing climate change. J. Paleolimnol. 40 (1), 273–293.
Larocque, I., Hall, R.I., Grahn, E., 2001. Chironomids as indicators of climate change: a 100-lake training set from a subarctic region of northern Sweden (Lapland). J. Paleolimnol. 26 (3), 307–322.
Lemdahl, G., 2000. Lateglacial and Early Holocene insect assemblages from sites at different altitudes in the Swiss Alps—implications on climate and environment. Palaeogeogr. Palaeoclimatol. Palaeoecol. 159 (3–4), 293–312.
Lischke, H., von Grafenstein, U., Ammann, B., 2013. Forest dynamics during the transition from the oldest dryas to the bølling–allerød at gerzensee—a simulation study. Palaeogeogr. Palaeoclimatol. Palaeoecol. 391, 60–73.
Litt, T., 1994. Paläoökologie, Paläobotanik und Stratigraphie des-Jungquartärs im nordmitteleuropäischen Tiefland: unter besonderer Berucksichtigung des Elbe-Saale-Gebietes. J. Cramer, Berlin-Stuttgart), p. 185.
Lods-Crozet, B., Lachavanne, J.B., 1994. Changes in the chironomid communities in Lake Geneva in relation with eutrophication, over a period of 60 years. Arch. Hydrobiol. 130 (4), 453–471.
Lotter, A.F., Walker, I.R., Brooks, S.J., Hofmann, W., 1999. An intercontinental comparison of chironomid palaeotemperature inference models: Europe vs North America. Quat. Sci. Rev. 18 (6), 717–735.
Lotter, A.F., Heiri, O., Brooks, S., van Leeuwen, J.F., Eicher, U., Ammann, B., 2012. Rapid summer temperature changes during Termination 1a: high-resolution multi-proxy climate reconstructions from Gerzensee (Switzerland). Quat. Sci. Rev. 36, 103–113.
Lowe, J.J., Rasmussen, S.O., Björck, S., Hoek, W.Z., Steffensen, J.P., Walker, M.J., Yu, Z.C., Intimate Group, 2008. Synchronisation of palaeoenvironmental events in the North Atlantic region during the Last Termination: a revised protocol recommended by the INTIMATE group. Quat. Sci. Rev. 27 (1–2), 6–17.
Luoto, T.P., 2009a. Subfossil Chironomidae (Insecta: Diptera) along a latitudinal gradient in Finland: development of a new temperature inference model. J. Quat. Sci. 24 (2), 150–158.
Luoto, T.P., 2009b. A Finnish chironomid-and chaoborid-based inference model for reconstructing past lake levels. Quat. Sci. Rev. 28 (15–16), 1481–1489.
Martinson, D.G., Pisias, N.G., Hays, J.D., Imbrie, J., Moore, T.C., Shackleton, N.J., 1987. Age dating and the orbital theory of the ice ages: development of a high-resolution 0 to 300,000-year chronostratigraphy 1. Quat. Res. 27 (1), 1–29.
Massaferro, J., Brooks, S.J., 2002. Response of chironomids to late quaternary environmental change in the taitao peninsula, southern Chile. J. Quat. Sci.: Published for the Quaternary Research Association 17 (2), 101–111.
McGarrigle, M.L., 1980. The distribution of chironomid communities and controlling sediment parameters in L. Derravaragh, Ireland. Chironomidae. Pergamon, pp. 275–282.
McManus, J.F., Bond, G.C., Broecker, W.S., Johnsen, S., Labeyrie, L., Higgins, S., 1994. High-resolution climate records from the North Atlantic during the last interglacial. Nature 371 (6495), 326–329.
Millet, L., Vannière, B., Verneaux, V., Magny, M., Disnar, J.R., Laggoun-Défarge, F., Walter-Simonnet, A.V., Bossuet, G., Ortu, E., de Beaulieu, J.L., 2007. Response of littoral chironomid communities and organic matter to late glacial lake—level, vegetation and climate changes at Lago dell'Accesa (Tuscany, Italy). J. Paleolimnol. 38 (4), 525–539.
Moore, J.W., 1974. Benthic algae of Southern Baffin Island: II. The epipelic communities in temporary ponds. J. Ecol. 809–819.
Moseley, G.E., Spötl, C., Brandstätter, S., Erhardt, T., Luetscher, M., Edwards, R.L., 2020. NALPS19: sub-orbital-scale climate variability recorded in northern Alpine speleothems during the last glacial period. Clim. Past 16 (1), 29–50.
Müller, U.C., 2000. A Late-Pleistocene pollen sequence from the Jammertal, southwestern Germany with particular reference to location and altitude as factors determining Eemian forest composition. Veg. Hist. Archaeobotany 9 (2), 125–131.
Müller, U.C., Pross, J., Bibus, E., 2003. Vegetation response to rapid climate change in Central Europe during the past 140,000 yr based on evidence from the Füramoos pollen record. Quat. Res. 59 (2), 235–245.
Nazarova, L., Self, A.E., Brooks, S.J., van Hardenbroek, M., Herzschuh, U., Diekmann, B., 2015. Northern Russian chironomid-based modern summer temperature data set and inference models. Global Planet. Change 134, 10–25.
Nazarova, L., Bleibtreu, A., Hoff, U., Dirksen, V., Diekmann, B., 2017. Changes in temperature and water depth of a small mountain lake during the past 3000 years in Central Kamchatka reflected by a chironomid record. Quat. Int. 447, 46–58.
North Greenland Ice Core Project members, 2004. High-resolution record of the Northern Hemisphere climate extending into the last interglacial period. Nature

431, 147–151.
Ponel, P., 1995. Rissian, eemian and würmian Coleoptera assemblages from La Grande pile (vosges, France). Palaeogeogr. Palaeoclimatol. Palaeoecol. 114 (1), 1–41.
Pope, R.J., Gordon, A.M., Kaushik, N.K., 1999. Leaf litter colonization by invertebrates in the littoral zone of a small oligotrophic lake. Hydrobiologia 392 (2), 99–112.
Porinchu, D.F., Cwynar, L.C., 2000. The distribution of freshwater Chironomidae (insecta: Diptera) across treeline near the lower lena river, northeast siberia, Russia. Arctic Antarct. Alpine Res. 32 (4), 429–437.
Preusser, F., Geyh, M.A., Schlüchter, C., 2003. Timing of Late Pleistocene climate change in lowland Switzerland. Quat. Sci. Rev. 22 (14), 1435–1445.
Rasmussen, S.O., Bigler, M., Blockley, S.P., Blunier, T., Buchardt, S.L., Clausen, H.B., Cvijanovic, I., Dahl-Jensen, D., Johnsen, S.J., Fischer, H., Gkinis, V., Guillevic, M., Hoek, W.Z., Lowe, J., Pedro, J., Popp, T., Seierstad, I., Steffensen, J., Svensson, A., Winstrup, M., 2014. A stratigraphic framework for abrupt climatic changes during the Last Glacial period based on three synchronized Greenland ice-core records: refining and extending the INTIMATE event stratigraphy. Quat. Sci. Rev. 106, 14–28.
Renssen, H., Isarin, R.F.B., 2001. The two major warming phases of the last deglaciation at~ 14.7 and~ 11.5 ka cal BP in Europe: climate reconstructions and AGCM experiments. Global Planet. Change 30 (1–2), 117–153.
RStudio Team, 2015. RStudio. Integrated Development for R. RStudio, Inc., Boston, MA. http://www.rstudio.com/.
Saether, O.A., 1979. Chironomid communities as water quality indicators. Ecography 2 (2), 65–74.
Samartin, S., Heiri, O., Vescovi, E., Brooks, S.J., Tinner, W., 2012. Lateglacial and early Holocene summer temperatures in the southern Swiss Alps reconstructed using fossil chironomids. J. Quat. Sci. 27 (3), 279–289.
Sánchez Goñi, M.F.S., Landais, A., Fletcher, W.J., Naughton, F., Desprat, S., Duprat, J., 2008. Contrasting impacts of Dansgaard–Oeschger events over a western European latitudinal transect modulated by orbital parameters. Quat. Sci. Rev. 27 (11–12), 1136–1151.
Sánchez Goñi, M.F.S., Bard, E., Landais, A., Rossignol, L., d'Errico, F., 2013. Air–sea temperature decoupling in western Europe during the last interglacial–glacial transition. Nat. Geosci. 6 (10), 837–841.
Schmid, P.E., 1993. A key to the larval Chironomidae and their instars from Austrian Danube region streams and rivers: with particular reference to a numerical taxonomic approach. 1. Diamesinae, Prodiamesinae and Orthocladiinae. Selbstverl.
Schreiner, A., 1981. Quartärgeologische Untersuchungen in der Umgebung von Interglazialvorkommen im östlichen Rheingletschergebiet (Baden-Württemberg).
Schreiner, A., 1996. Erläuterungen zu 8025 Bad Wurzach: Geologische Karte von Baden- Württemberg 1:25 000. In: Landesvermessungsamt Baden-Württemberg, Freiburg, first ed.
Seguinot, J., Ivy-Ochs, S., Jouvet, G., Huss, M., Funk, M., Preusser, F., 2018. Modelling last glacial cycle ice dynamics in the Alps. Cryosphere 12 (10), 3265–3285.
Shackleton, N.J., Sánchez-Goñi, M.F., Pailler, D., Lancelot, Y., 2003. Marine isotope substage 5e and the Eemian interglacial. Global Planet. Change 36 (3), 151–155.
Šmilauer, P., Lepš, J., 2014. Multivariate Analysis of Ecological Data Using CANOCO 5. Cambridge University Press.
Solhøy, T., 2001. Oribatid mites. In: Smol, J.P., Birks, H.J.B., Last, W.M. (Eds.), Tracking Environmental Change Using Lake Sediments Volume 4 Zoological Indicators, vol. 4. Kluwer Academic Publishers, Dordrecht, pp. 81–104.
Spratt, R.M., Lisiecki, L.E., 2016. A Late Pleistocene sea level stack. Clim. Past 12 (4), 1079–1092.
Stockmarr, J.A., 1971. Tablets with spores used in absolute pollen analysis. Pollen Spores 13, 615–621.
Tóth, M., Magyari, E.K., Brooks, S.J., Braun, M., Buczkó, K., Bálint, M., Heiri, O., 2012. A chironomid-based reconstruction of late glacial summer temperatures in the southern Carpathians (Romania). Quat. Res. 77 (1), 122–131.
Tóth, M., Magyari, E.K., Buczkó, K., Braun, M., Panagiotopoulos, K., Heiri, O., 2015. Chironomid-inferred Holocene temperature changes in the south carpathians (Romania). Holocene 25 (4), 569–582.
Tóth, M., van Hardenbroek, M., Bleicher, N., Heiri, O., 2019. Pronounced early human impact on lakeshore environments documented by aquatic invertebrate remains in waterlogged Neolithic settlement deposits. Quat. Sci. Rev. 205, 126–142.
Vandekerkhove, J., Declerck, S., Vanhove, M., Brendonck, L., Jeppesen, E., Conde Porcuna, J.M., De Meester, L., 2004. Use of ephippial morphology to assess richness of anomopods: potentials and pitfalls. J. Limnol. 63 (1s), 75–84.
Waelbroeck, C., Labeyrie, L., Michel, E., Duplessy, J.C., McManus, J.F., Lambeck, K., Balbon, E., Labracherie, M., 2002. Sea-level and deep water temperature changes derived from benthic foraminifera isotopic records. Quat. Sci. Rev. 21 (1–3), 295–305.
Walker, I.R., MacDonald, G.M., 1995. Distributions of Chironomidae (Insecta: Diptera) and other freshwater midges with respect to treeline, Northwest Territories, Canada. Arct. Alp. Res. 27, 258–263.
Walker, I.R., Smol, J.P., Engstrom, D.R., Birks, H.J.B., 1991. An assessment of Chironomidae as quantitative indicators of past climatic change. Can. J. Fish. Aquat. Sci. 48 (6), 975–987.
Walkling, A.P., Coope, G.R., 1996. Climatic reconstructions from the eemian/early weichselian transition in central Europe based on the coleopteran record from gröbern, Germany. Boreas 25 (3), 145–159.
Wiederholm, T., 1983. Chironomidae of the Holarctic Region. Keys and Diagnoses. Part 1. Larvae. 67, vol. 457. Entomologica Scandinavica.
Winterholler, K., 2004. Zur jungpleistozänen landschaftsentwicklung am füramooser ried (oberschwaben). In: Beiträge zur Geomorphologie, Bodengeographie und Quartärforschung. Geographischen Institut der Universität Tübingen, pp. 155–180.
Woillard, G.M., 1978. Grande Pile peat bog: a continuous pollen record for the last 140,000 years. Quat. Res. 9 (1), 1–21.
Wulf, S., Hardiman, M.J., Staff, R.A., Koutsodendris, A., Appelt, O., Blockley, S.P., Lowe, J.J., Manning, C.J., Ottolini, L., Schmitt, A.K., Smith, V.C., Tomlinson, E.I., Vakhrameeva, P., Knipping, M., Kotthoff, U., Milner, A.M., Christanis, K., Kalaitzidis, S., Tzedakis, P.C., Schmiedl, G., Pross, J., 2018. The marine isotope stage 1–5 cryptotephra record of Tenaghi Philippon, Greece: towards a detailed tephrostratigraphic framework for the Eastern Mediterranean region. Quat. Sci. Rev. 186, 236–262.